Available online at www.sciencedirect.com
SCIENCE DIRECT
Journal of Power Sources 150 (2005) 150–181
JOURNAL OF POWER SOURCES
www.elsevier.com/locate/jpowsour

Switching to a U.S. hydrogen fuel cell vehicle fleet: The resultant change in emissions, energy use, and greenhouse gases

W.G. Colella [a,*], M.Z. Jacobson [a], D.M. Golden [b]

[a] *Department of Civil and Environmental Engineering, Stanford University, Stanford, CA 94305, USA*
[b] *Department of Mechanical Engineering, Stanford University, Stanford, CA 94305, USA*

Received 29 December 2004; received in revised form 30 May 2005; accepted 30 May 2005
Available online 10 August 2005

Abstract

This study examines the potential change in primary emissions and energy use from replacing the current U.S. fleet of fossil-fuel on-road vehicles (FFOV) with hybrid electric fossil fuel vehicles or hydrogen fuel cell vehicles (HFCV). Emissions and energy usage are analyzed for three different HFCV scenarios, with hydrogen produced from: (1) steam reforming of natural gas, (2) electrolysis powered by wind energy, and (3) coal gasification. With the U.S. EPA's National Emission Inventory as the baseline, other emission inventories are created using a life cycle assessment (LCA) of alternative fuel supply chains. For a range of reasonable HFCV efficiencies and methods of producing hydrogen, we find that the replacement of FFOV with HFCV significantly reduces emission associated with air pollution, compared even with a switch to hybrids. All HFCV scenarios decrease net air pollution emission, including nitrogen oxides, volatile organic compounds, particulate matter, ammonia, and carbon monoxide. These reductions are achieved with hydrogen production from either a fossil fuel source such as natural gas or a renewable source such as wind. Furthermore, replacing FFOV with hybrids or HFCV with hydrogen derived from natural gas, wind or coal may reduce the global warming impact of greenhouse gases and particles (measured in carbon dioxide equivalent emission) by 6, 14, 23, and 1%, respectively. Finally, even if HFCV are fueled by a fossil fuel such as natural gas, if no carbon is sequestered during hydrogen production, and 1% of methane in the feedstock gas is leaked to the environment, natural gas HFCV still may achieve a significant reduction in greenhouse gas and air pollution emission over FFOV.

Keywords: Hydrogen fuel cell vehicle; Life cycle assessment; Air pollution; Coal gasification; Steam reforming; Wind electrolysis

1. Introduction

The purpose of this analysis is to study the potential effects on air pollution and global climate of replacing fossil-fuel on-road vehicles (FFOV) with those powered by hydrogen fuel cells, where the hydrogen is produced from: (1) steam reforming of natural gas, (2) wind-powered electrolysis, or (3) coal gasification. The present paper conducts a well-to-wheels analysis for different hydrogen fuel cell vehicle (HFCV) scenarios and determines the net changes in primary emissions and energy use that result. The emission results from this study serve as inputs into a second study, which examines the effect of these emission changes on ambient air pollution and on potential health and climate costs [1]. The complete research effort is published in two parts in these two separate papers.

This paper combines a life cycle assessment (LCA) with data from the U.S. Environmental Protection Agency's (EPA's) National Emission Inventory (NEI) [2] to estimate the net change in emission upon a switch to a hybrid FFOV or a HFCV fleet. We evaluate one hybrid FFOV scenario and three HFCV scenarios in which hydrogen is produced by: (1) decentralized steam reforming of natural gas, (2) decentralized electrolysis powered by wind turbines, and (3) centralized coal gasification [3]. We conduct a LCA of different HFCV scenarios to evaluate the primary energy and pollutant flows involved in fossil fuel and hydrogen scenarios

* Corresponding author. Tel.: +1 650 283 2701; fax: +1 501 629 2818.
E-mail address: wcolella@alumni.princeton.edu (W.G. Colella).

0378-7753/$ – see front matter © 2005 Published by Elsevier B.V.
doi:10.1016/j.jpowsour.2005.05.092

during fuel extraction, production, transport, storage, delivery, and use on the vehicle (the fuel supply chain). In cases where a range of performance assumptions are plausible, we use conservative assumptions to strengthen the credibility of the final results. This study uses the NEI as input for the atmospheric model to verify the model's resultant concentrations of air pollutants against measured values for the base case of a 1999 vehicle fleet. We combine the results of the LCA with the NEI by developing alternative emission inventories that reflect changes in the LCA under different hydrogen production scenarios. These alternative emission inventories record the actual emission of gases and particle components associated with hydrogen fuel production and use and the corresponding change in emissions associated with reducing fossil fuel use. They serve as the primary inputs to an atmospheric model in the second paper, which examines the effects of changes in emission on air pollution using a three-dimensional numerical model of the atmosphere and ocean (GATOR-GCMOM) [4,5]. Model results are compared with paired-in-time-and-space data here.

To date, several studies have examined the economics, the environmental impacts, and the safety of using hydrogen as a fuel for vehicles. A DOE study investigated the economics of different methods of producing hydrogen for vehicles from renewable sources [6]. The study analyzed the economic and physical feasibility of producing enough hydrogen (10 quads) to supply a 2003-sized vehicle fleet in the year 2004 from renewable electricity sources, in particular, biomass, wind, solar photovoltaic, and geothermal. The study concluded that, among these sources, the most economically attractive and physically available renewable energy resource is wind power, potentially contributing 70% of the total energy required across the U.S., and at 40% lower cost than solar photovoltaic. The study also concluded that, in such a future scenario, Class 4 wind resources (ranging between 5.6 and 6.0 m s^{-1} winds at 10 m) may be more highly utilized than Class 5 (6.0–6.4 m s^{-1} winds at 10 m) or Class 6 (6.4–7.0 m s^{-1} winds at 10 m) resources because of their proximity to population centers and consequent lower transmission costs. The greater feasibility of Wind Class 4-generated hydrogen to a future HFCV fleet underscores the importance of investigating this scenario for the study. Kartha estimates that hydrogen derived from electrolysis will cost between $2.75 and $4.50 per gasoline-gallon equivalent of H_2 for electricity purchased at between 0.04 and 0.08 cents $(kW\,h)^{-1}$, respectively [7]. Bauen et al. demonstrates significant greenhouse gas reductions with hydrogen produced from wind for vehicles [8]. Studies by the DOE, NASA, and the California Fuel Cell Vehicle Partnership have concluded that hydrogen can be used safely as a fuel for vehicles following certain guidelines [9].

Other studies have highlighted scenarios for a hydrogen economy that are either energy inefficient or produce high levels of pollution. One energy inefficient, highly pollutive scenario involves the use of gasoline-to-hydrogen fuel reformers onboard the vehicle [10,11]. Most automakers have abandoned programs to develop this technology [12,13]. Another energy inefficient and pollutive scenario involves electrolyzing water to produce hydrogen with electricity provided by the current mix of stationary power plants [14]. The same European Union study determined that the HFCV would produce less greenhouse gas emissions and would be more energy efficient from well-to-wheels than hydrogen internal combustion engine (ICE) vehicles. Another promoted but inefficient hydrogen economy scenario involves: (1) the production of liquid hydrogen fuel (which consumes 30% of the heating value of the fuel), (2) trucking it to distribution centers, and (3) using it to fuel ICE (which operate at lower efficiencies than fuel cells and produce NO_x emissions) [15]. Other studies underestimate the relative well-to-wheel efficiency improvement and emission reductions with HFCV [16,17]. By contrast, our study demonstrates energy efficient and low emission scenarios for a hydrogen economy based on the use of gaseous hydrogen and fuel cells.

In addition, several studies have examined specific aspects of the potential impact of a hydrogen economy on the ozone layer, greenhouse gases, and air pollution [18–20]. However, these studies did not examine the net change in emission resulting from a switch to a hydrogen economy resolved down to the county or state level. They also did not perform a life cycle assessment to examine the net changes in emissions resulting from different methods of producing hydrogen. By contrast, this study addresses this change by combining LCA with the NEI.

2. Methodology

This paper conducts a LCA for: (1) the current 1999 FFOV fleet, (2) a hybrid-fossil fuel electric scenario, and (3) three different HFCV scenarios. For each scenario, the primary energy and pollutant flows are analyzed across the fuel supply chain. This paper combines the results of the LCA with the NEI by developing alternative emission inventories that reflect changes in the LCA under different hydrogen production scenarios. This paper also compares the atmospheric model's predictions of ambient pollutant concentrations with measured values. We discuss: (1) the LCA methodology, (2) the NEI, and (3) the combined LCA and NEI analysis for the five scenarios.

2.1. Life cycle assessment

LCA was used to examine the primary mass, energy, and pollutant flows involved in each hydrogen production scenario [21]. LCA uses mass and energy balance calculations to analyze the net pollutant and energy flows crossing a control volume around the primary fuel supply chain, a methodology similar to analysis of a process plant. The primary fuel supply chain for vehicles includes fuel extraction, production, transport, storage, delivery, and use onboard the vehicle. LCA examines this fuel supply chain from "well-to-

wheels." Within this chain, LCA focuses on the most energy and pollution-intensive links [22].

Figs. 1 through 4 illustrate LCA for the base case of the conventional FFOV fleet and for three different HFCV scenarios. Fig. 1 shows a LCA for the conventional 1999 on-road vehicle fleet, which consumes primarily gasoline and diesel fuel within internal combustion engines (ICE). Fig. 2 shows a LCA for a HFCV scenario with the hydrogen derived from natural gas. Figs. 3 and 4 show the same supply chain with the hydrogen derived from wind and coal, respectively. The analysis of these LCA is discussed in subsequent sections.

2.2. U.S. Environmental Protection Agency's (EPA's) National Emission Inventory (NEI)

The U.S. EPA's NEI estimates air pollution emissions from all U.S. anthropogenic sources, including vehicles, power plants, boilers, manufacturing facilities, and industrial facilities, for every year since 1989, and also for 1980 and 1985, by county. The inventory considers 370,000 stack and fugitive sources, 250,000 area sources, and 1700 categories of on-road and non-road vehicular sources (including 837 categories of gasoline vehicles).

Table 1 shows NEI emission estimates for 1999 for broad categories: (1) on-road vehicles, (2) non-road mobile sources, (3) point and area sources that include power plants, and (4) total emissions from anthropogenic sources (the sum of each of the three prior categories). On-road vehicles include motorcycles, passenger vehicles, trucks, recreational vehicles, etc. Non-road mobile sources include lawn mowers, tractors, construction vehicles, farm vehicles, industrial vehicles, etc. Point and area sources include electric power plants, chemical processing plants, heating equipment, etc. Because the estimates shown in Table 1 include emission estimates from the conventional fossil fuel on-road vehicle fleet, these data comprise the base case used in this analysis.

As reflected in Table 1, the NEI estimates gas and particle emissions. Gases accounted for include carbon monoxide (CO), ammonia (NH_3), speciated nitrogen oxides (NO_x), speciated sulfur oxides (SO_x), and organics. Speciated NO_x includes nitrogen oxide (NO), nitrogen dioxide (NO_2), and nitrous acid (HONO). Speciated SO_x includes sulfur dioxide (SO_2) and sulfur trioxide (SO_3). Additional gases include organic compounds such as paraffin carbon (PAR), olefin carbon (OLE), ethylene (C_2H_4), formaldehyde (HCHO), acetaldehyde (CH_3CHO), toluene (TOL), xylene (XYL), isoprene (ISOP), non-reactive hydrocarbons/methane (NR/CH_4). The inventory treats both fine particulate matter ($PM_{2.5}$), which is 2.5 μm in diameter and smaller, and course particulate matter (PM_{10}), which is 10 μm in diameter and less and includes $PM_{2.5}$. Speciated particle matter (PM) include organic matter ($OM_{2.5}$ and OM_{10}), black carbon ($BC_{2.5}$ and BC_{10}), sulfate ($SULF_{2.5}$ and $SULF_{10}$), nitrate ($NIT_{2.5}$ and NIT_{10}), and other particle matter ($OTH_{2.5}$ and OTH_{10}).

Table 1 also shows emission estimates of other species not recorded in the NEI: (1) hydrogen (H_2), (2) carbon dioxide (CO_2), and (3) water vapor (H_2O). These emission rates were derived from other emissions in the NEI and conservation of mass calculations, described below.

In the base case (1999 fossil fuel vehicles), the primary source of H_2 emissions is incomplete combustion. Because H_2 and CO are both products of incomplete combustion, they tend to be emitted proportionally to one another. As shown in Table 1, CO emissions are listed in the NEI. The quantity of H_2 emission was derived from the quantity of CO, assuming 0.029 units of mass of H_2 per unit of mass of CO for combustion processes [23]. In later HFCV scenarios, the quantity of H_2 emission also includes estimates of leaked H_2.

CO_2 emissions were based on fuel consumption and CO_2 emission factors shown in Table 2. For vehicles, total CO_2 emissions were a product of the total distance driven and a CO_2 emission factor for the average vehicle of 320 g CO_2 km^{-1}, shown in Table 2. This CO_2 emission factor for the average vehicle was based on rescaling an emission factor of 38 g C km^{-1} for a vehicle with a fuel consumption of 39 miles $gallon^{-1}$ for a vehicle with the average fuel consumption of the U.S. fleet, 17.11 miles $gallon^{-1}$. For power plants, total CO_2 emissions were a product of the total amount of fuel consumed by a particular type of power plant and CO_2 emission factors for each type of fuel, as shown in Table 2.

Water vapor emissions were based on different molar ratios of H_2O to CO_2 emission during combustion of various fuels. For on-road vehicles, the quantity of water vapor emitted was based on the stoichiometric combustion of a combination of gasoline and light diesel fuel ($C_nH_{1.85n}$), which yields a molar ratio of H_2O to CO_2 of 0.93. For electric power plants, the quantity of water vapor emitted was based on the weighted average for natural gas and coal plants, assuming the current mix of U.S. electric generation plants (52% coal and 16% natural gas). Stoichiometric combustion leads to a molar ratio of H_2O to CO_2 of 1.2 for coal and 2 for methane (approximating natural gas), such that the weighted average of these for all power plants is 0.92 moles of H_2O to CO_2. For the category of other sources in Table 1, the same conversion factor was applied.

Emissions from each source and location were allocated in time (with 1-h resolution) with U.S. EPA temporal emission factors. The raw emissions for stack and fugitive sources were given by actual location of emission. Area and mobile emissions were allocated by county; however, they were distributed spatially within each county by spatial surrogate factors, including population, roads, agriculture, households, ports, airports, and railroads.

2.3. Base case: 1999 gasoline and diesel internal combustion engine vehicle fleet

Table 1 summarizes emissions for the base case scenario, which assumes a 1999 ICE fleet. The current ICE vehicle fleet is chosen as a base case instead of a potential future

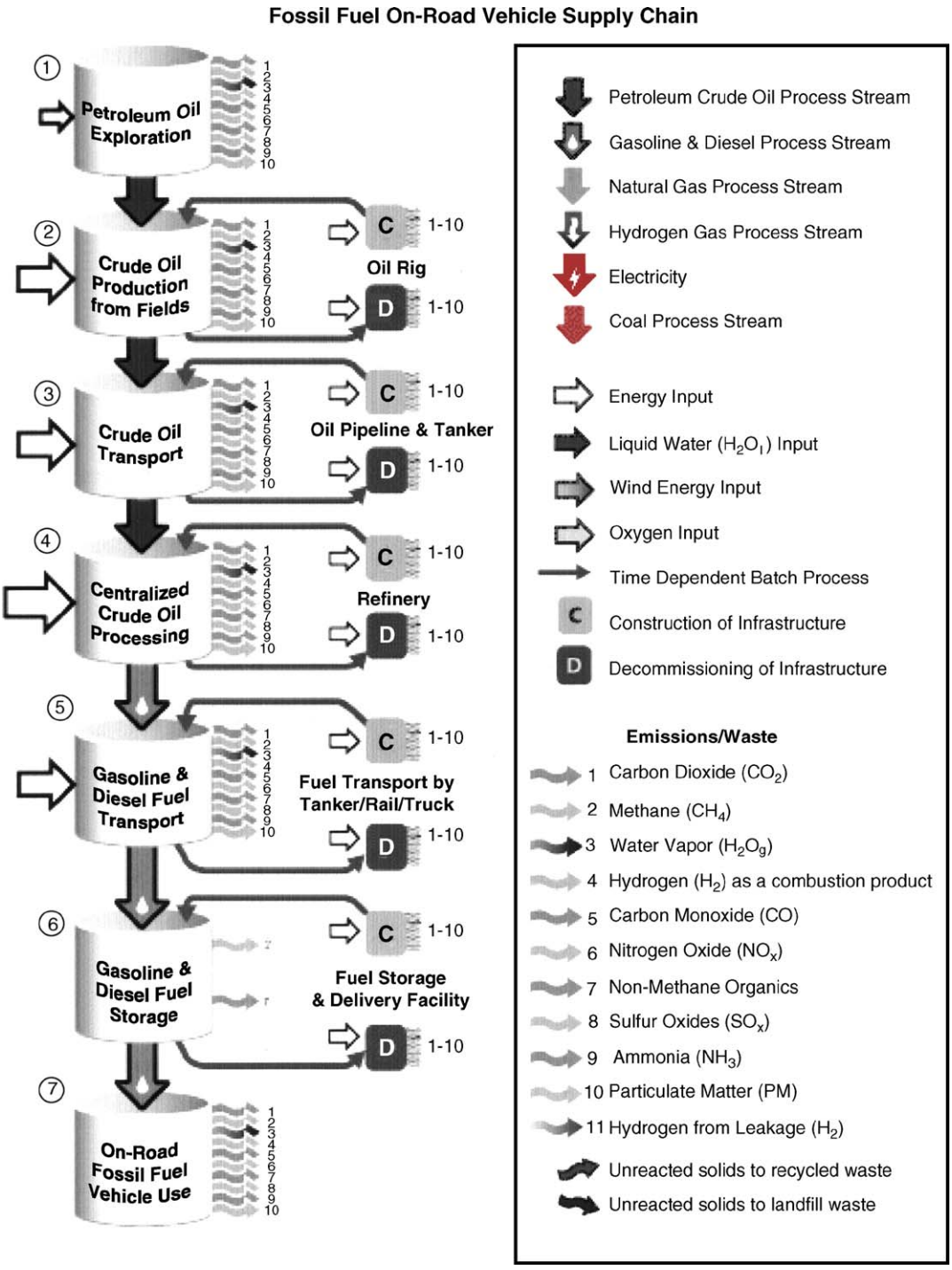

Fig. 1. Life cycle analysis (LCA) supply chain for the conventional 1999 gasoline and diesel on-road vehicle fleet using internal combustion engines (ICE). Along the supply chain from fuel extraction to consumption, the supply chain shows the energy inputs and emission outputs along the entire chain from "well-to-wheels." The process stream arrows show the flow of the working fluid (the primary fuel) as it is transformed. The cylinders 1–7 indicate processes on the working fluid from its extraction, to its refining, to its end use in the vehicle. The curved arrows show emissions released during each process. Emissions 1–10 are released during the combustion of fossil fuels related to processes 1 through 5 and 7. Process 6 (fuel storage) emits small quantities of methane and non-methane organics through fuel vaporization and subsequent leakage, but requires negligible energy. The solid white arrows show the energy requirements for each process; the relative sizes of these arrows with respect to each other approximately indicate the relative amount of energy required for each process. The most energy intensive process along the chain is the centralized processing of crude oil into refined gasoline and diesel fuels, followed by oil extraction from fields and crude or refined fuel transport. The primary supply chain is shown on the left with cylinders 1–7. Secondary supply chains are shown on the right, which involve the construction and decommissioning of related infrastructure. While the primary chain refers to a continuous process, the secondary supply chains are composed of a series of one-off batch processes, such as the construction and decommissioning of a gasoline station (secondary supply chain of cylinder 6). Related emission and energy inputs are also shown. Legend for Figs. 1–4 is shown in the box.

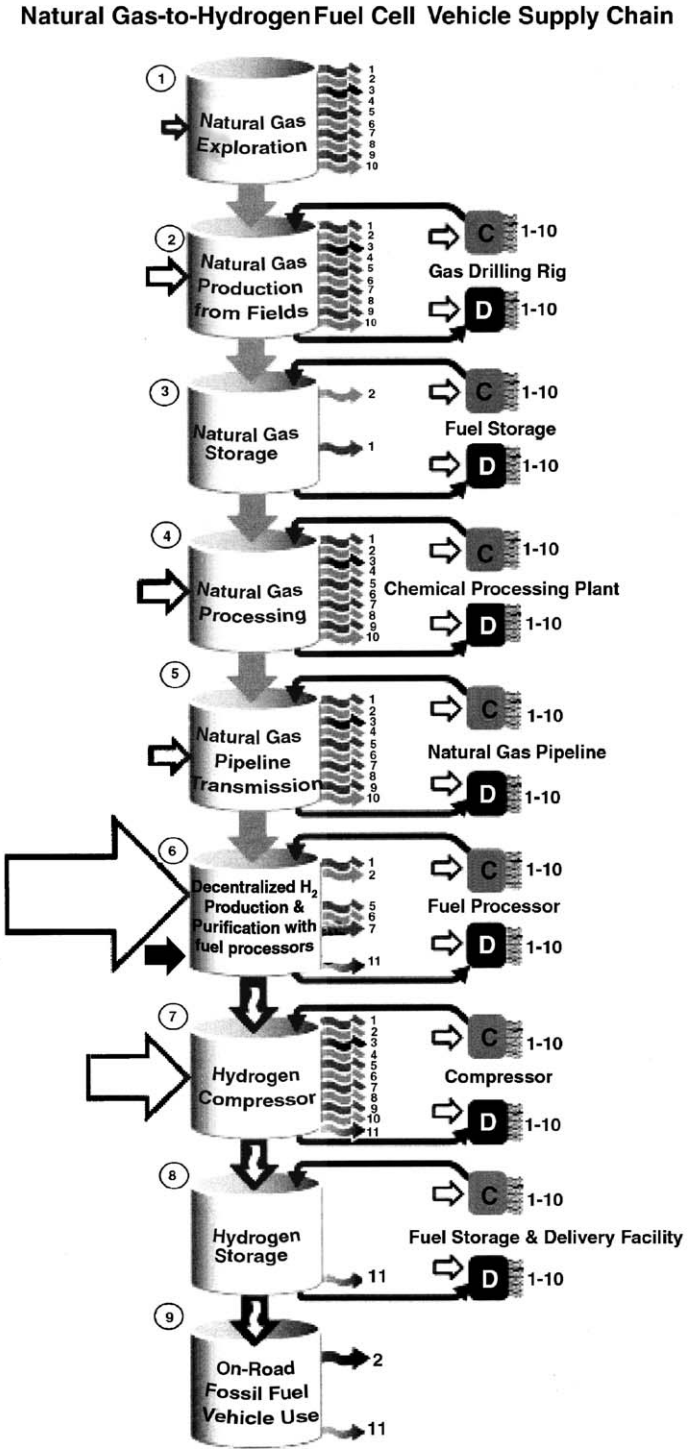

Fig. 2. Life cycle analysis (LCA) supply chain for hydrogen fuel cell vehicles (HFCV) with hydrogen derived from natural gas. Processes 1, 2, 4, and 5 release combustion emissions 1 through 10 during related transport, power generation, and/or chemical processing. Process 3 releases methane and non-methane organics through natural gas leakage. Process 6 releases CO_2, CH_4, CO, NO_x, non-methane organics, and H_2 emissions. Process 6 is also the most energy intensive. Process 7 releases combustion emissions 1 through 10 because the electricity required to run the compressors is assumed to arise from the current mix of electricity generators. Process 7 is the second most energy intensive process in the chain. Processes 7, 8 and 9 emit H_2 through leakage. In process 9, hydrogen vehicles emit water vapor during use, though this vapor could be condensed to liquid form. Within the figure, the relative sizes of the energy input arrows approximate the relative amount of energy required for each process. The secondary supply chains, shown on the right, require energy and produce emissions. However, an assumption of this analysis is that the energy requirements and emissions produced by the secondary supply chains in one scenario are roughly equivalent to those in another scenario, and, in comparisons, cancel each other out. For legend, please see Fig. 1.

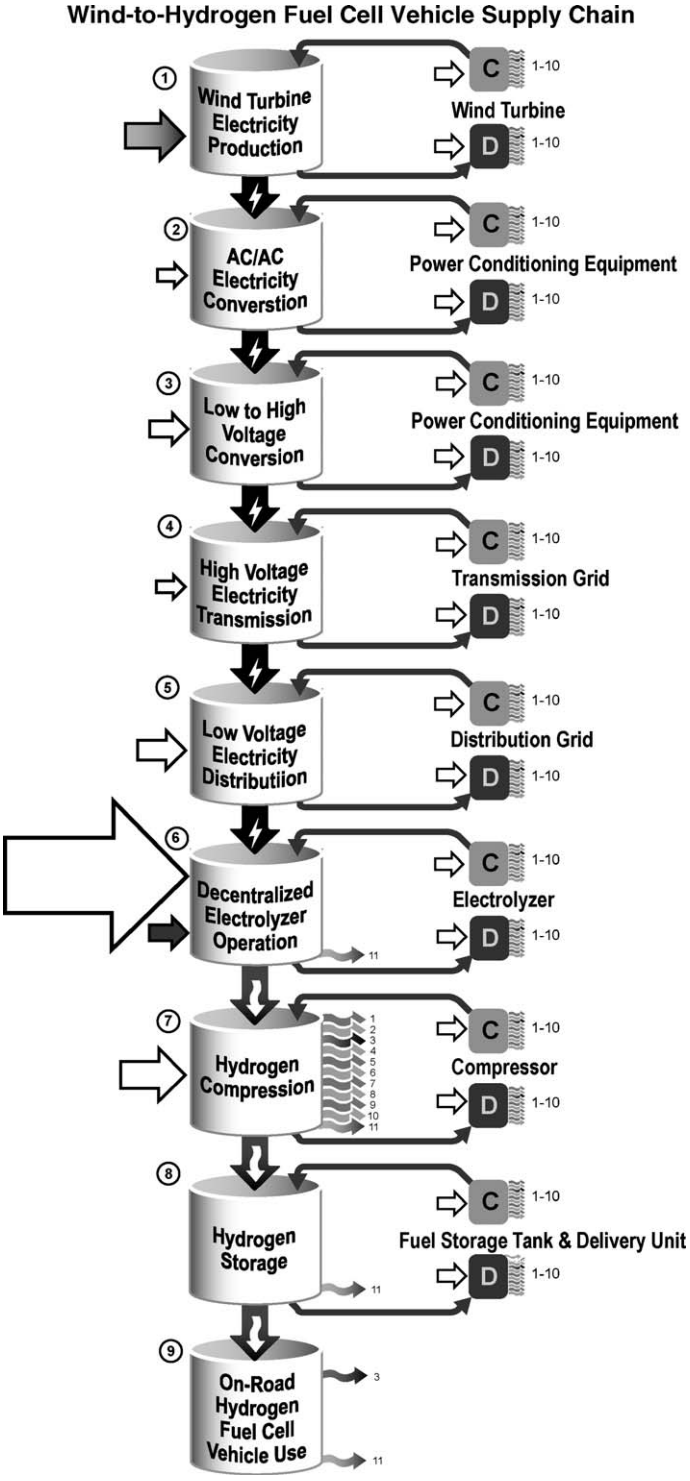

Fig. 3. Life cycle analysis (LCA) supply chain for hydrogen fuel cell vehicles (HFCV) with hydrogen derived from wind. Process 7 releases combustion emissions during compression of hydrogen powered by the current mix of electricity generating plant (52% coal). However, this process requires a fraction of energy compared with the electrolyzer (5% of electrical consumption at the electrolyzer). Hydrogen is released here both through leakage and through incomplete combustion at the upstream power plants. Processes 6–9 release H_2 emission through leakage. Process 6 is the most energy intensive and consumes liquid water. In process 9, hydrogen vehicles emit water vapor during use, though this vapor could be condensed to liquid form. Within the figure, the relative sizes of the energy input arrows approximate the relative amount of energy required for each process. The secondary supply chains, shown on the right, require energy and produce emissions. However, an assumption of this analysis is that the energy requirements and emissions produced by the secondary supply chains in one scenario are roughly equivalent to those in another scenario, and, in comparisons, cancel each other out. For legend, please see Fig. 1.

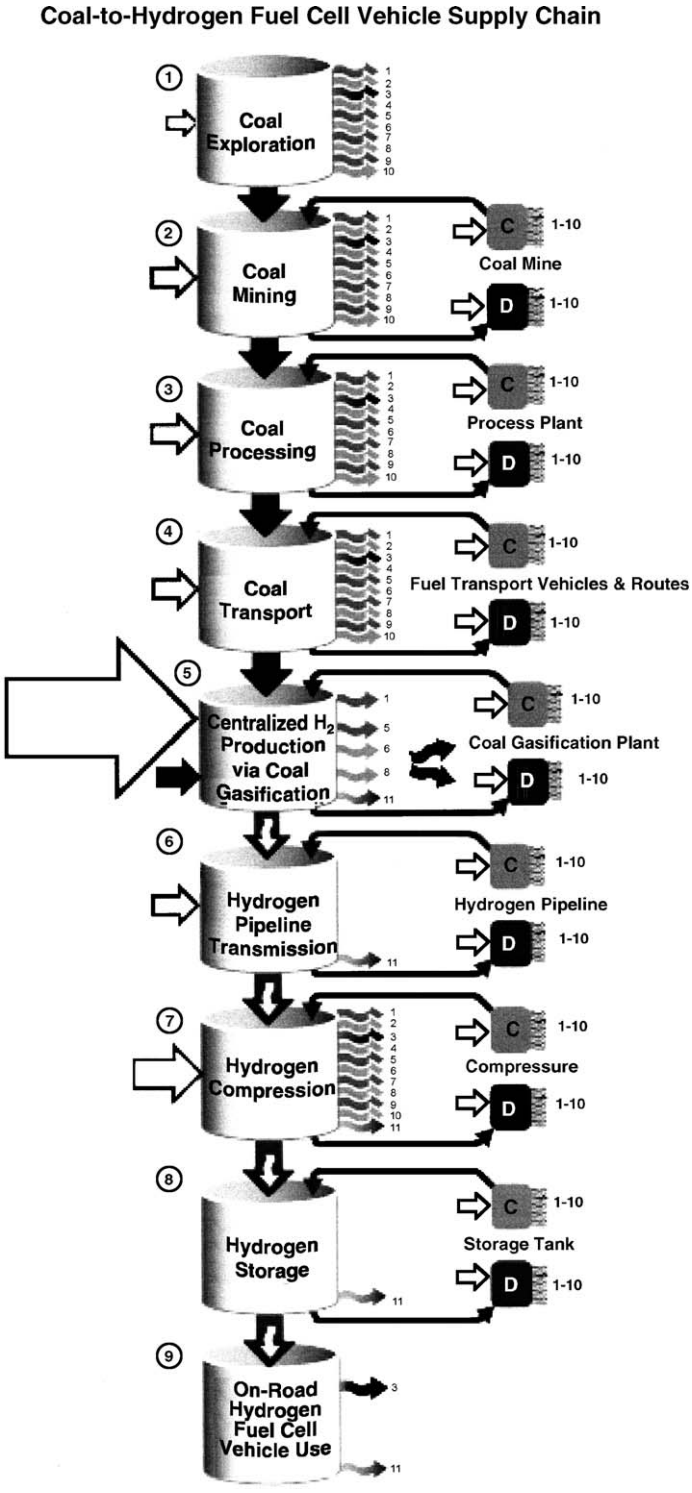

Fig. 4. Life cycle analysis (LCA) supply chain for hydrogen fuel cell vehicles (HFCV) with hydrogen derived from coal. Processes 1–4 and 7 release combustion emissions 1 through 10 during related fuel transport, power generation, and/or chemical processing. Process 5, coal gasification, releases CO_2, CO, NO_x, SO_x and H_2 through leakage. This process is the most energy intensive, and consumes O_2 and liquid water. Additional waste from process 5 includes unreacted solids that become recycled waste and landfill waste. Process 7 releases combustion emissions 1 through 10 because the electricity required to run the compressors is assumed to arise from the current mix of electricity generators. Process 7 is the second most energy intensive process in the chain. Processes 5–9 emit H_2 through leakage. In process 9, hydrogen vehicles emit water vapor during use, though this vapor could be condensed to liquid form. Within the figure, the relative sizes of the energy input arrows approximate the relative amount of energy required for each process. The secondary supply chains, shown on the right, in one scenario require energy and produce emissions. However, an assumption of this analysis is that the energy requirements and emissions produced by the secondary supply chains in one scenario are roughly equivalent to those produced in another scenario, and, in comparisons, cancel each other out. For legend, please see Fig. 1.

Table 1
Base case with fossil fuel on-road vehicle (FFOV) fleet emission production (metric ton year^{-1})

Species	On-road vehicles	Non-road mobile sources	Point and area sources including electric power plants	Total
Gases				
Carbon monoxide (CO)	6.18E+07	2.28E+07	2.71 E+07	1.12E+08
Nitrogen oxides (NO_x) as NO_2	7.57E+06	4.02E+06	1.03E+07	2.19E+07
Organics				
Paraffins (PAR)	3.53E+06	1.74E+06	8.75E+06	1.40E+07
Olefins (OLE)	1.61E+05	8.53E+04	2.75E+05	5.21E+05
Ethylene (C_2H_4)	2.27E+05	1.27E+05	5.58E+05	9.12E+05
Formaldehyde (HCHO)	4.43E+04	4.91 E+04	1.29E+05	2.23E+05
Higher aldehydes (ALD2)	1.72E+05	9.36E+04	7.34E+04	3.39E+05
Toluene (TOL)	3.29E+05	1.63E+05	2.11E+06	2.60E+06
Xylene (XYL)	4.66E+05	2.19E+05	1.56E+06	2.25E+06
Isoprene (ISOP)	4.86E+03	2.05E+03	3.01 E+03	9.92E+03
Total non-methane organics	4.93E+06	2.48E+06	1.35E+07	2.09E+07
Methane (CH_4)	7.91 E+05	4.24E+05	5.10E+06	6.31 E+06
Sulfur oxides (SO_x) as SO_2	2.72E+05	4.31 E+05	1.74E+07	1.81 E+07
Ammonia (NH_3)	2.39E+05	3.19E+04	4.26E+06	4.53E+06
Hydrogen (H_2)	1.76E+06	6.49E+05	7.74E+05	3.18E+06
Particulate matter				
Organic matter ($OM_{2.5}$)	5.04E+04	8.89E+04	2.50E+06	2.64E+06
Black carbon ($BC_{2.5}$)	9.07E+04	1.32E+05	3.69E+05	5.92E+05
Sulfate ($SULF_{2.5}$)	1.88E+03	6.20E+03	3.02E+05	3.10E+05
Nitrate ($NIT_{2.5}$)	2.47E+02	7.03E+02	2.58E+04	2.67E+04
Other ($OTH_{2.5}$)	2.40E+04	6.19E+04	8.17E+06	8.26E+06
Total $PM_{2.5}$	1.67E+05	2.90E+05	1.14E+07	1.18E+07
Organic matter (OM_{10})	7.19E+04	9.75E+04	5.60E+06	5.77E+06
Black carbon (BC_{10})	1.07E+05	1.44E+05	7.10E+05	9.62E+05
Sulfate ($SULF_{10}$)	2.99E+03	6.72E+03	4.82E+05	4.91 E+05
Nitrate (NIT_{10})	3.15E+02	7.72E+02	6.99E+04	7.10E+04
Other (OTH_{10})	3.66E+04	6.40E+04	3.74E+07	3.75E+07
Total PM_{10}	2.19E+05	3.13E+05	4.43E+07	4.48E+07
Species	On-road vehicles	Other sources	Electric power plants	Total
Carbon dioxide (CO_2)	1.37E+09	1.70E+09	2.23E+09	5.30E+09
Water (H_2O)	5.19E+08	6.38E+08	8.38E+08	1.99E+09
CO_2 equivalent (low)	1.36E+09	1.70E+09	2.27E+09	5.33E+09
CO_2 equivalent (high)	1.39E+09	1.74E+09	2.72E+09	5.86E+09

On-road vehicles include motorcycles, passenger vehicles, trucks, recreational vehicles, etc. Non-road mobile sources include lawn mowers, tractors, construction vehicles, farm vehicles, industrial vehicles, etc. Point and area sources include electric power plants, chemical processing plants, heating equipment, etc. Source for all emissions except H_2, CO_2, and H_2O is the U.S. National Emission Inventory (NEI), http://www.epa.gov/ttn/chief/net/1999inventorv.html. H_2, CO_2, and H_2O emissions derived from CO emissions and fuel use, as described in the main text.

ICE vehicle fleet based on more modernized, fuel efficient vehicles for four main reasons. First, the performance of the 1999 FFOV fleet can be quantitatively described by the NEI's extensive mobile sources database, which details emissions and fuel economy [24]. Second, using 1999 emissions data permits verification of the atmospheric model via comparisons of the model's resultant concentrations of air pollution with measured values. Verification of the atmospheric model is shown shortly. Third, although more modern, fuel efficient ICEs exist, the U.S. trend in fuel economy over the past 20 years has not been toward more fuel efficient vehicles. The average fuel economy of cars and trucks declined between the late 1980s and the late 1990s, and has remained constant since then at 6% less than its peak [25]. Therefore, a future ICE vehicle fleet cannot be expected to be necessarily more fuel efficient than the 1999 fleet. Fourth, technology analysts and business economists would estimate that ICE vehicles appear to be approaching the end of their product development cycle. Without a paradigm-shift to a new type of technology (such as a hybrid electric drive train or an ultra-light weight composite chassis), conventional ICE vehicles can be expected to achieve only modest increases in fuel economy over previous years. Nevertheless, we include a hybrid case here to account for the possibility of a modernized ICE fleet.

2.3.1. Base case verification of atmospheric model against measured emissions

For the 1999 base case scenario, Fig. 5a–o compares atmospheric model predictions with paired-in-time-and-space August 1999 data for meteorological, radiation, gas, and

Table 2
CO_2 emission factors

Average vehicle in 1999 U.S. fleet (kg CO_2 km^{-1})	0.318
Electric power plants	
Coal (kg CO_2 kg^{-1} coal)	2.14
Natural gas (kg CO_2 m^{-3} natural gas)	0.00193
Oil (kg CO_2 kg^{-1} oil)	3.11
Liquid petroleum gas (LPG) (kg CO_2 kg^{-1} LPG)	2.77
Wood (kg CO_2 kg^{-1} wood)	1.65

aerosol parameters in the U.S. grid. A paired-in-time-and-space comparison is one in which model predictions are compared with data values at the exact locations and times of the measurement. Paired-in-time-and-space comparisons are the most rigorous type of model evaluation possible. Parameters compared included: (a) air pressure, (b) temperature, (c) relative humidity, (d) wind speed and direction, (e) surface solar irradiance, (f) surface UV radiation, (g) ozone, (h) ethane, (i) propane, (j) toluene, (k) isoprene, (1)

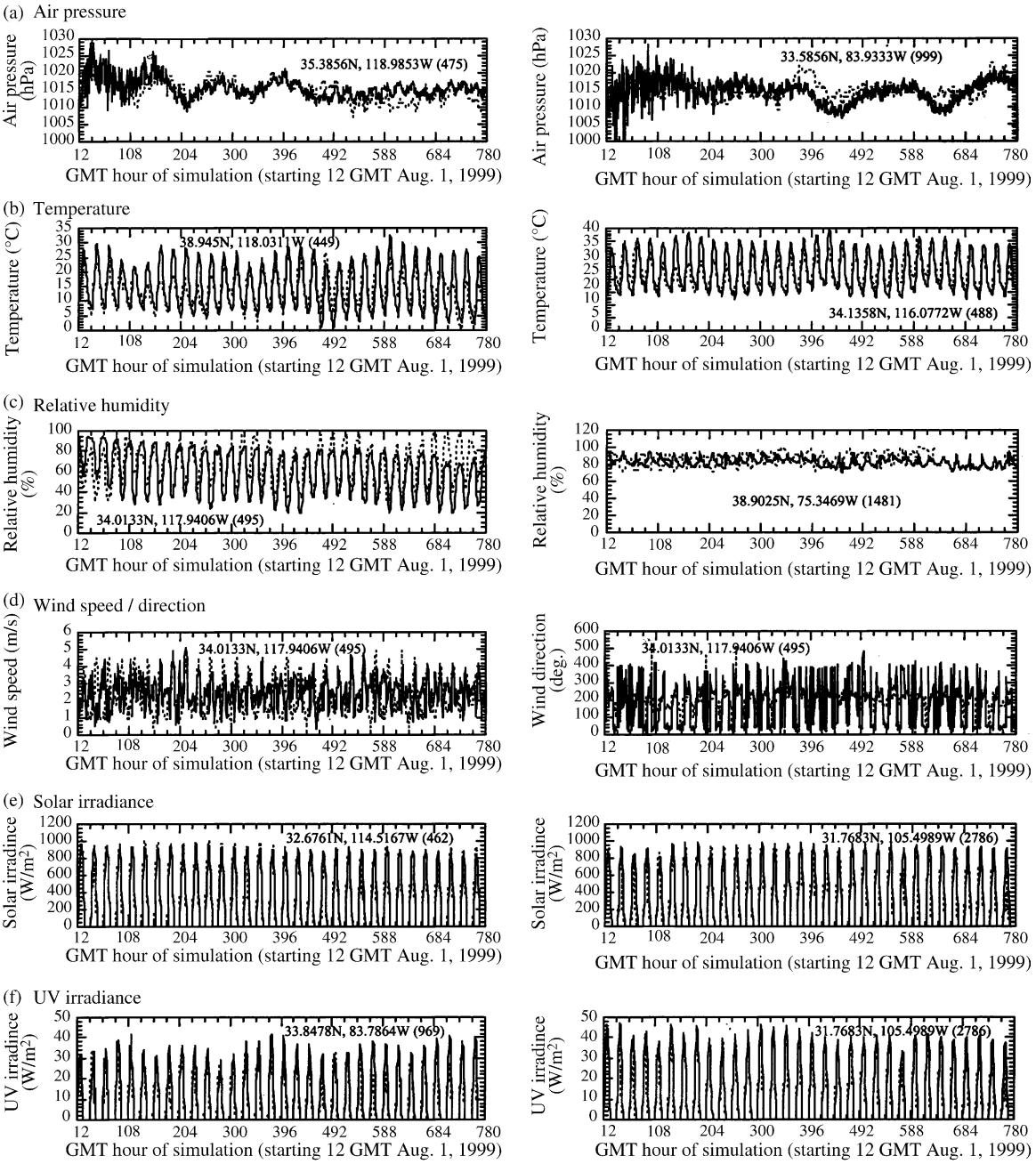

Fig. 5. Comparison of atmospheric model output (solid lines) with measured data (dashed lines) for ambient air pollution and environmental conditions. Comparisons are shown for a random sample of different locations, with the latitude and longitude of each location shown. Locations selected at random. Ambient air pollution data is from U.S. EPA AIR Data, http://www.epa.gov\air\data.

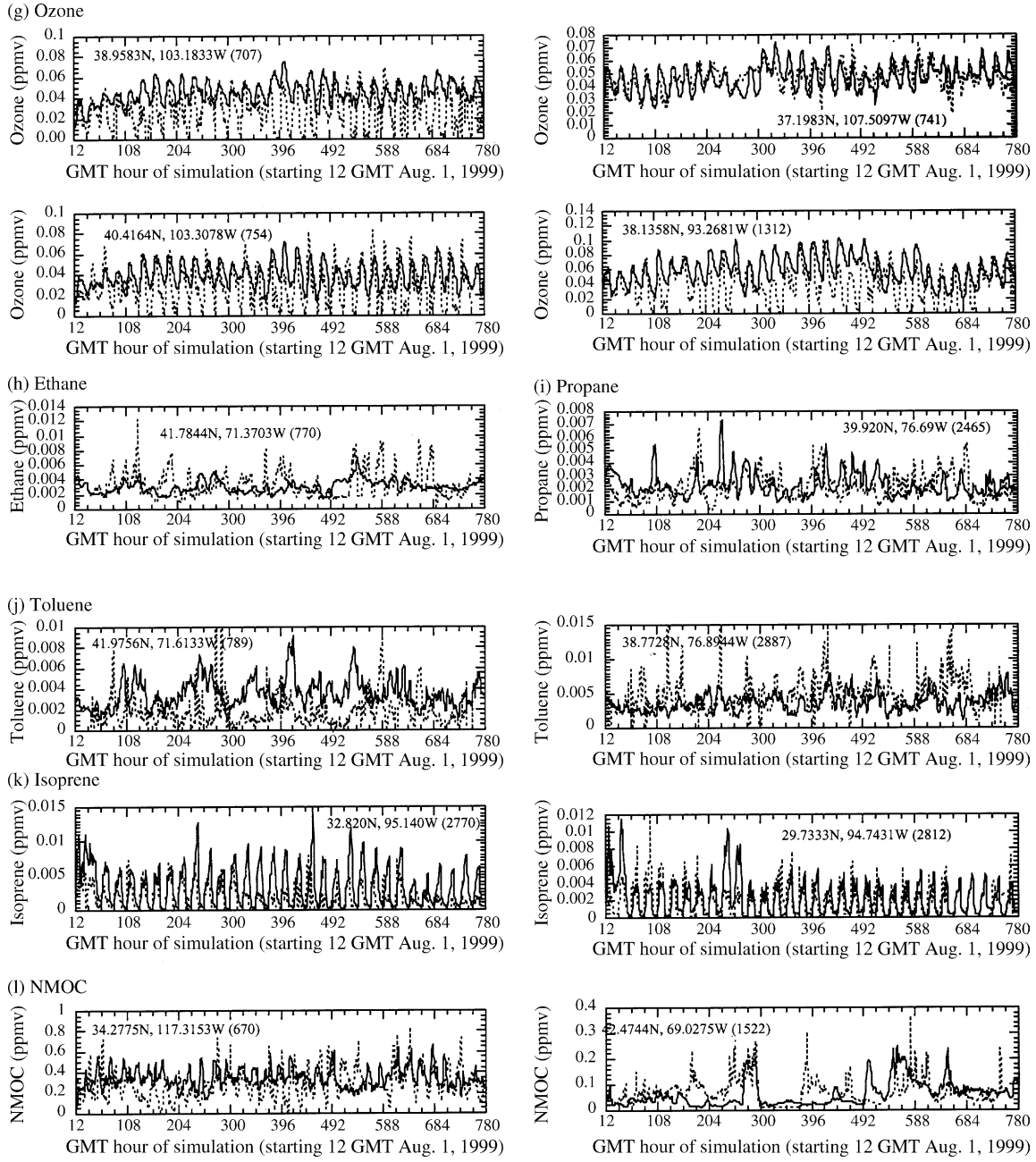

Fig. 5. (*Continued*)

non-methane organic carbon (NMOC), (m) nitrogen dioxide, (n) carbon monoxide, and (o) particles smaller than 10 μm in diameter (PM_{10}). The time resolution of the data (and model output) was 1 h in all cases. No data assimilation, nudging, or model spinup was performed during the model simulation. Model results were interpolated with bilinear interpolation from four surrounding grid cell centers to the exact location of the measurement. Data were from the U.S. EPA AIR Data [26]. The number in parentheses is the station identifier. The atmospheric model used for this study is described in detail in the accompanying paper [1] and elsewhere.[4,5]

2.4. Common assumptions for the hybrid and fuel cell scenarios

In the hybrid and HFCV scenarios, several common assumptions are made. First, the replacement of 100% of conventional FFOV is assumed to occur instantaneously in one year, 1999. This replacement is not a practical strategy for phasing in a new vehicle fleet, but rather a heuristic exercise from which we can learn about the relative change in emissions. Second, scenarios were designed to consider the more economically attractive configurations within a technology type. For example, decentralized natural gas steam

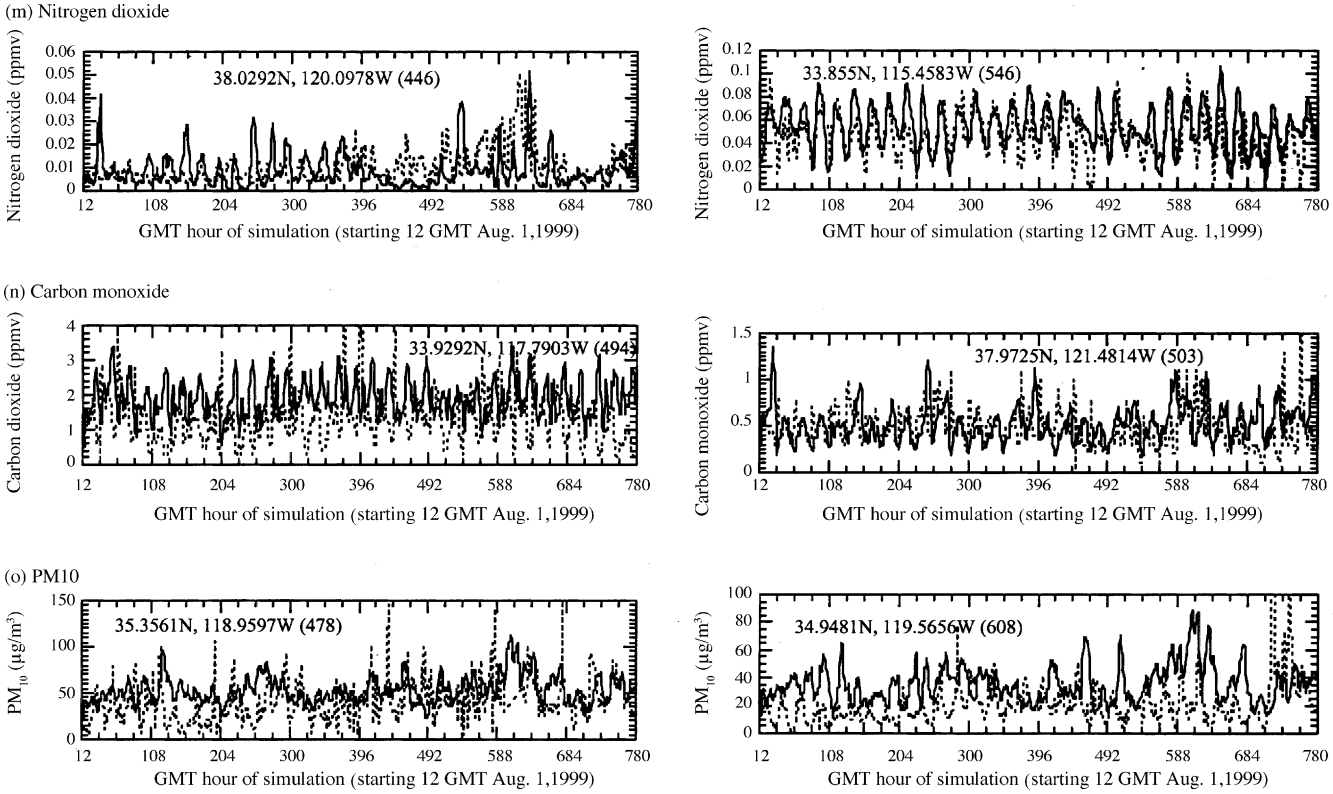

Fig. 5. (*Continued*).

reformers were considered over centralized ones because decentralized units could rely on the current natural gas distribution pipelines whereas centralized ones would require building an extensive network of new pipelines for carrying hydrogen. Third, the scenarios differ in their commercial readiness-to-market, with hybrid electric vehicles closest to commercialization followed by HFCV powered by natural gas, wind, and coal, in that order. Among these, the coal scenario might require the longest and most financially intensive research and development effort, in part because no advanced coal gasification plant has been built specifically for hydrogen production to date. Despite these differences in readiness-to-market and required research and development investment time, all scenarios were considered ready for implementation at the same time. Fourth, in all scenarios, the vehicles require the same motive force. Equivalent motive power signifies that the hybrid or HFCV fleet has the same distributions of vehicle mass, aerodynamic drag, rolling resistance, frontal area, and wheel-assembly rotating inertia as the 1999 fleet, as well as being subject to the same drive cycles [27]. The vehicle chasses remain the same, and only the power systems are replaced. Fifth, the power and fueling systems are similar in weight, such that one can replace the other.

Sixth, Figs. 1 through 4 show secondary supply chains to the right of each primary supply chain. These secondary supply chains consist of the construction and decommissioning of infrastructure needed for the primary supply chain. As shown in Fig. 1, secondary supply chains include the construction and decommissioning of: (1) oil rigs needed for production, (2) oil pipelines and tankers needed for crude oil transport, (3) refineries for centralized crude oil processing, (4) oil tankers, railroads, and trucks for refined fuel transport, and (5) fuel storage and fuel station delivery infrastructure. Each of these secondary supply chains consumes energy and produces emissions. However, an assumption of this analysis is that the energy requirements and emissions produced by secondary supply chains in one scenario are roughly equivalent to those in other scenarios. As a result, in comparing scenarios, the environmental and energy impacts of secondary supply chains roughly cancel out. These secondary supply chains are also considered the least significant for their environmental and energy impacts because they primary consist of a series of batch processes rather than a continuous process as in the primary supply chain. This assumption is consistent with the findings of other LCA studies. For example, in an LCA of hydrogen production via natural gas steam reforming, Spath estimates that the global warming contribution for constructing and decommissioning of both steam reforming plants and natural gas pipelines combined was 0.4% of the total across the supply chain [28]. As a result of being primarily batch processes, these secondary supply chains are assumed negligible in this analysis.

Finally, technological performance is based on the most advanced 2005 prototypes for which information has been made publicly available, for technologies all along the hybrid and fuel cell supply chains (shown Figs. 2–4). Performance

data for HFCV is given in the subsequent section "Comparison of Conventional FFOV Efficiency with HFCV Efficiency." Unlike ICEs, fuel cell systems are at the beginning of their product development cycle, and therefore, given appropriate incentives for innovation, can be expected to achieve more dramatic gains in their performance than ICEs. Therefore, the peak performance achieved by pre-commercial fuel cell systems in 2005 is assumed to characterize the average performance of fuel cell systems in the future. Unlike other studies that hypothesize the potential future performance of energy technologies, this study bases its performance assumptions on manufacturers' best current prototypes.

2.4.1. Upstream energy use and emissions

A gasoline fuel supply chain is composed of similar process steps as the hydrogen fuel supply chain, including exploration, production, processing and refining, and fuel transport via trucks, tankers, or pipeline. From well-to-tank, the gasoline supply chain consumes approximately 12% of the energy in its fuel [29]. For comparison, in the natural gas supply chain, approximately 10% of the lower heating value (LHV) chemical energy in the natural gas fuel is needed during the: (1) exploration (0.7%), (2) production (5.6%), (3) storage and processing (1.0%), and (4) transmission (2.7%) of the gas [30]. The same supply chain is relied on in a natural gas HFCV scenario. The fuel supply chain stages for coal used in industrial power plants are approximately equal to those stages used prior to coal consumption in centralized gasification plants, with approximately the same energy requirements as gasoline and natural gas during these stages. Due to similarities in the energy requirements of these separate sections of fuel supply chains, the upstream energy requirements in the gasoline fuel cycle are equated with the energy requirements in the hydrogen fuel cycle between well-and-tank with the exception of: (1) hydrogen production (the creation of hydrogen fuel from another fuel source) and (2) hydrogen compression. These energy requirements were added onto the energy requirements of the HFCV scenarios.

The gasoline cycle produces evaporative emissions of volatile organic compounds and combustion emissions of several pollutants (NO_x, CO, HCs, CO, PM). In the HFCV scenarios, where gasoline emissions were replaced with hydrogen emissions, evaporative and combustion-related emissions related to petroleum production for vehicle transport were eliminated in the U.S. NEI. For example, half of VOC emissions created in petroleum production were eliminated in proportion to the percentage of petroleum production related to vehicle fuels. In the hybrid case, these emissions were reduced in proportion to the reduction in fuel consumption.

2.5. Scenario 1: gasoline hybrid electric ICE vehicle scenario

The hybrid fleet was modeled as a more efficient version of the 1999 FFOV fleet. It was modeled to have the same emission factors per unit mass of fuel consumed as the 1999 FFOV but less fuel consumption per mile traveled. The fleet-averaged energy efficiency increase upon conversion of FFOV to hybrid vehicles was estimated as 45%, corresponding to a 31% emission decrease (1/1.5) [31].

The hybrid fleet was assumed to have the same pollutant emission factors per mass of fuel consumed as the FFOV for several reasons. Some of the newest hybrid vehicles qualify as partial zero emission vehicles (PZEV), i.e. the California Air Resources Board (CARB) has sanctioned them as having extremely clean tailpipe standard meeting the super ultra low emission vehicle (SULEV) standard [32]. However, these vehicles have qualified as PZEV not because they are hybrids (not because they employ a hybrid vehicle drive train composed of an engine and electrical storage device), but rather because of the additional pollution control technology added to them by manufacturers. By itself, conversion from a conventional vehicle drive train to a hybrid one primarily improves vehicle efficiency, not emission factors per unit of fuel consumed. Second, this future hybrid fleet may have a similar distribution of gasoline and diesel vehicles as the 1999 FFOV, with the fuel type being a primary determinant of the emission factor. Finally, although emission factors from some new FFOV vehicles will be lower than current emission factors, the fleet average emissions may not decrease as significantly since the introduction of the lowest emission hybrid vehicles may not be uniform and the effect of new pollution control technology often diminishes with a car's age. In this study, we compared the fleet average hybrid against the fleet average HFCV.

2.6. Overview of hydrogen fuel cell vehicle fleet supply chain scenarios

This section gives an overview of some of the common points of investigation surrounding all HFCV scenarios. First, this section gives an overview of the change in emissions in the HFCV scenarios. Second, this section discusses the derivation of hydrogen consumption by HFCV. Finally, this section discusses hydrogen compression for onboard vehicle storage, hydrogen leakage in the fuel supply chain, and emissions released during the incremental consumption of grid electrical power.

2.6.1. Overview of change in emissions in HFCV scenarios

For the scenario in which the U.S. vehicle fleet is converted to HFCV, all gas and particle emissions in the U.S. inventory associated with vehicles (including vehicle emissions (pollutants and water vapor), refinery emissions, and pipeline emissions) were eliminated from the simulations, and emissions arising from hydrogen fuel cell vehicle use were added. In the case where steam reforming of methane was considered, emissions included hydrogen leaks, water vapor emission, methane combustion emission (due to generation of heat for steam reformation), methane leaks during

distribution and processing, and emission due to compressing and transporting hydrogen. When coal gasification was used to generate hydrogen, emissions included CO_2, CO, leaked H_2, some residual SO_2 and NO_x, and all products of coal cracking required to raise the temperature and pressure during the coal gasification process. Emissions resulting from the manufacture of steam-reforming plants, coal gasification plants, and wind turbines were also considered. In all cases, changes in location of emissions were treated as follows: The location and magnitude of emissions from existing natural gas and coal-fired power plants were accounted for in the NEI. New power generation for hydrogen generation based on the current mix of power plants was assumed to occur in the same locations as current power generation. The location of emissions from centralized coal gasification plants was assumed to be the same location as current coal power plants for electric power production (recorded in the NEI). The location of emissions from distributed natural gas steam reformers was assumed to be the same location as current gasoline refueling stations. Vehicle emissions were assumed to occur in the same location as with the NEI 1999 fleet.

2.6.2. Hydrogen consumption by vehicles

The quantity of hydrogen-related emission is ultimately a function of the projected hydrogen consumption in on-road vehicles. Data for hydrogen consumption from on-road vehicles was derived by taking the distance driven in each U.S. county in 1999 from the U.S. NEI, then converting the mileage into energy requirements for propelling these vehicles (using the average fleet mileage of all on-road vehicles in the NEI's 1999 database of 17.11 miles gallon^{-1} [33] and an average FFOV efficiency of 16% based on the lower heating value (LHV) chemical energy in the fuel), and converting the energy required for propelling the vehicles into hydrogen requirements based on an average hydrogen LHV vehicle efficiency of 46%. Fig. 6 shows the resulting estimated annual hydrogen fuel consumption by county in the U.S. due to the replacement of all FFOV with HFCV. In total, HFCV would consume about 57 megatonnes (MT) H_2 year^{-1}. On average, each person would consume 200 kg of H_2 year^{-1} for on-road transportation. Current U.S. production is about 8 MT H_2 year^{-1} and global production is about 50 MT H_2 year [34].

The mass of hydrogen consumed by vehicles per county per year (m_{H_2C}) depends on the number of vehicle miles traveled per county per year (V_{MT}) and the fuel consumption rate for HFCV (F_h), according to

$$m_{H_2C} = \frac{V_{MT}}{F_h}, \quad (1)$$

where

$$F_h = \frac{(\bar{M}_{gvf} V_c L_h \eta_h)}{(\rho_g L_g \eta_g)}.$$

In these equations, m_{H_2C} is the mass of hydrogen consumed by vehicles per county per year (10^6 kg year^{-1}), V_{MT} the vehicle miles traveled per year per county (10^6 miles), F_h the fuel consumption for HFCV (miles kg H_2^{-1}), $\bar{M}_{gvf}$ the average mileage of the conventional FFOV fleet (miles gallon^{-1}) = 17.11 miles gallon^{-1}, V_c the volumetric conversion (gallons m^{-3}) = 260 gallons m^{-3}, ρ_g the density of gasoline (kg m^{-3}) = 750 kg/m^3 [35], L_g the lower heating value of gasoline fuel (MJ kg^{-1}) = 44 MJ kg^{-3}, L_h the lower heating value of hydrogen fuel (MJ kg^{-1}) = 120 MJ kg^{-3}, η_g the conventional FFOV efficiency = vehicle's motive energy/LHV of fuel = 0.16, η_h the HFCV efficiency = vehicle's motive energy/LHV of fuel = 0.46.

2.6.2.1. Comparison of conventional FFOV efficiency with HFCV efficiency. Vehicle efficiency is defined as the ratio of the amount of motive energy used to propel a vehicle to the amount of LHV chemical energy in the fuel. It is a complex function of: (1) the efficiency of the power system (i.e. the engine or the fuel cell system), (2) the efficiency of subsystems such as power conversion, (3) the efficiency of the transmission, and (4) the efficiency of the drive train. Most important, vehicle efficiency is a function of the vehicle's drive cycle, the record of how a vehicle's speed changes with time. The vehicle's speed impacts its efficiency because the power system and transmission efficiency depend on their required output. For ICE vehicles, engine efficiency varies with engine speed and required torque (or load). The engine has an efficiency "sweet-spot" over a small range of speeds and torques where efficiency is highest. The transmission efficiency also varies with load. The manner in which engines vary in efficiency with load differs significantly for fuel cell systems. For these reasons, vehicle efficiency depends strongly on the driving patterns of the vehicle.

The average vehicle efficiency (η_g) across the 1999 U.S. FFOV fleet is estimated to be 16%. This value is based on performance data of a Ford Motor Company ICE passenger vehicle with the same average mileage as that of the U.S. fleet and on the simulation of this vehicle's performance over a typical U.S. driving cycle [36]. Our study assumes similar vehicle performance as the Ford study: an average engine efficiency of 20% (ratio of mechanical work output of crankshaft/LHV of fuel) and an average mechanical drive train efficiency of 80% (ratio of effective motive energy of the vehicle/mechanical output of engines) [37], giving an overall vehicle efficiency of 16% (0.20×0.80). This value of 16% precisely concurs with an estimate by Toyota Motor Corporation for the current fleet [38]. For comparison, Honda R&D estimates the efficiency of its newest FFOV tested against the U.S. EPA's City Driving Cycle at 22% [39,40]. (Also for comparison, the Ford study showed that it is more efficient from well-to-wheels to convert natural gas into hydrogen for use onboard a HFCV than to use natural gas fuel directly in an ICE because of the higher efficiency of the fuel cell system over that of the ICE and the high conversion of efficiency of natural gas to hydrogen.) [41]

The average vehicle efficiency (η_h) of a HFCV fleet is estimated to be 46%. The η_h can be estimated from the fuel

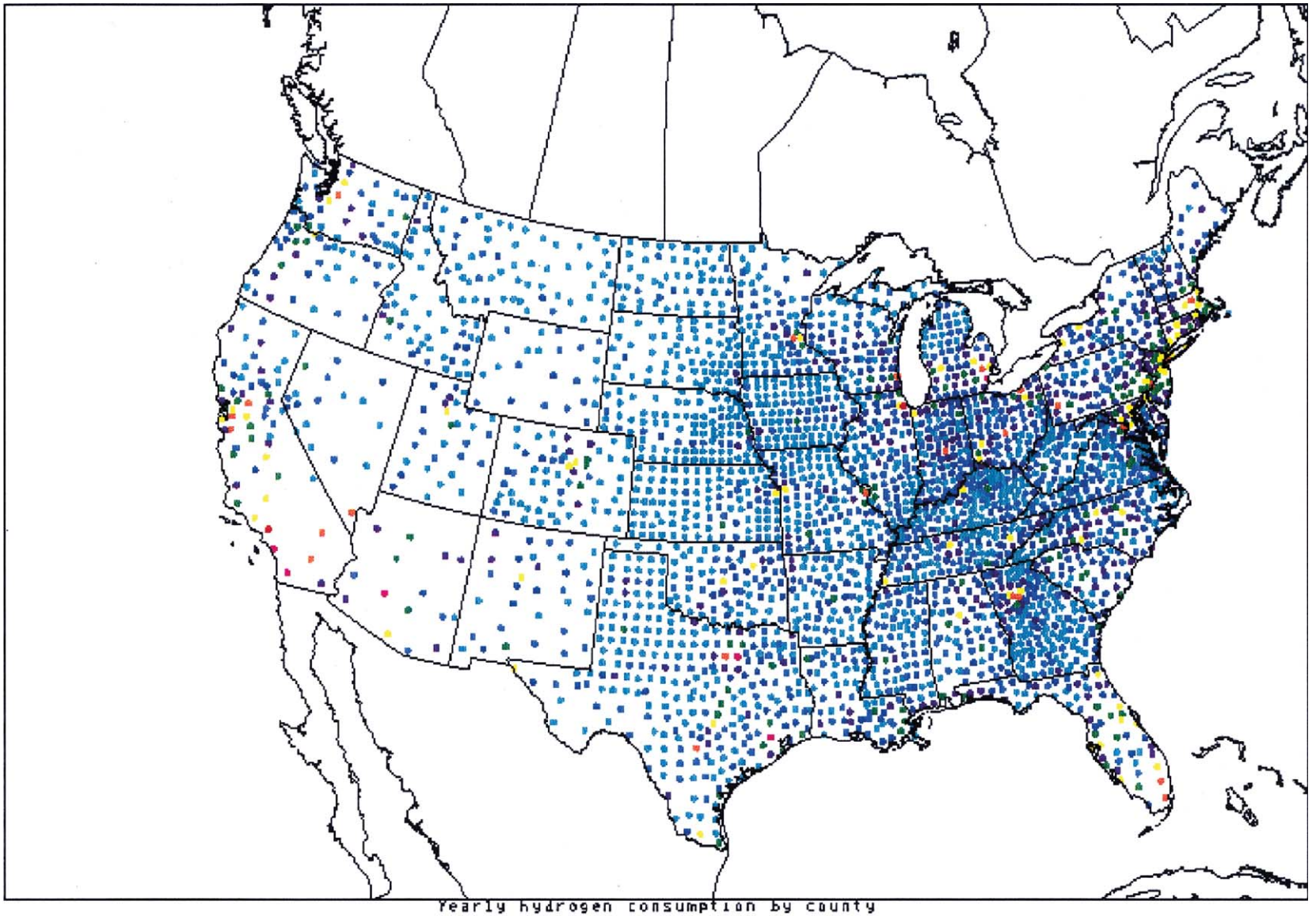

Fig. 6. Spatial distribution of estimated annual hydrogen fuel consumption by county in the United States resulting from the replacement of all fossil fuel on-road vehicles (FFOV) with hydrogen fuel-cell vehicles (HFCV). H_2 consumption per county plotted at the center of each county. Because U.S. counties in the West tend to be larger in area than those in the East, the lower density of dots in the West indicates fewer counties with a larger area. (Legend in kton year^{-1}: light blue = 0–5; medium blue = 5–10; dark blue = 10–20; purple = 20–40; green = 40–80; yellow = 80–160; orange = l 60–320; magenta = 320–640; red > 640 kton year^{-1}; 1 kton = 1E3 metric ton.) On-road vehicles would consume approximately 57 megatonnes (MT) of hydrogen fuel per year. (For interpretation of the references to colour in this figure legend, the reader is referred to the web version of the article.)

cell system efficiency (η_s), the inverter efficiency (η_i), and electric motor efficiency (η_m), according to

$$\eta_h = \eta_s \, \eta_i \, \eta_m \quad (2)$$

The fuel cell system efficiency (η_s) is the net quantity of DC electrical power produced by the fuel cell power system per unit of hydrogen fuel input. The inverter efficiency (η_i) is the net quantity of AC electric power exiting the inverter per unit of DC electrical power received from the fuel cell system. The electric motor efficiency (η_m) is the mechanical output power of the motor for propelling the vehicle per unit of AC electrical power input from the inverter. The fuel cell company Ballard produces hydrogen fuel cell systems for automotive use with a maximum efficiency of 48% (electrical output from the system/LHV of hydrogen fuel) [42]. Ballard also produces inverters for fuel cell systems on board vehicles which have an efficiency of 98% [43]. Premium electric motors can achieve efficiencies as high as 97%. Multiplying these three values leads to an estimated vehicle efficiency range of 46%. Toyota reports a tank-to-wheel efficiency of their prototype HFCV of 50% [44]. Honda R&D reports a tank-to-wheel efficiency for its 2005 ultra capacitor-assisted *FCX* prototype HFCV of greater than 50%, tested against the U.S. EPA's City Driving Cycle [40,45,46]. Because these efficiencies are based on published product data sheets and industrial data from tested vehicles, they are very reasonable estimates of the best performance of a future HFCV. As such, the use of an efficiency of 46% may be conservative. Fig. 7 compares the tank-to-wheels vehicle efficiency for three types of Honda vehicles tested against the EPA's City Driving Cycle: (1) a 2005 standard FFOV, (2) a 2005 hybrid FFOV, and (3) a 2005 HFCV prototype.

A ratio of HFCV efficiency to FFOV efficiency of 2.9 (46%/16%) is within the range of reasonable estimates. As emphasized by the 2004 NRC Report on Hydrogen, because fuel cells are in their technological infancy in their development cycle, their efficiency can not be predicted accurately, only estimated [47]. A detailed computer simulation study by Directed Technologies tested a natural gas-fueled ICE vehicle and HFCV performance against different drive cycles, each of which emphasize various types of driving conditions (such as city or highway driving.) [48] The study concluded that the ratio of HFCV efficiency to FFOV efficiency could vary over a range between 1.8 and 3.7. The value of 2.9 is close to the median of this range. Toyota has stated that the ratio of their prototype HFCV's efficiency to the current fleets FFOV efficiency is 3.1, and they intend to achieve a ratio of 3.8 for future prototypes [49]. Based on a literature review of fuel cell efficiencies by Wang et. al, comparing advanced ICE vehicles (not the current fleet) with HFCV, the 2004 National Research Council report on the Hydrogen Economy assumes a ratio of 2.4:1 [50]. Comparing advanced ICE vehicles (not the current fleet) and HFCV, the Rocky Mountain Institute also estimates an efficiency ratio of 2.4 [51]. However, all of these estimates could be considered on the lower end of the potential gain in fuel economy because they do not take into account potential gains from a switch to a more modern "hyper-car" vehicle design, employing light-weight composite materials and low aerodynamic drag so as to reduce the required motive force of the vehicle [52]. In analyzing the relative ratio of HFCV and FFOV efficiencies, one of the variables that would impact this ratio the most (through a sensitivity analysis) is the type of drive cycle they are subjected to.

2.6.3. Hydrogen compression for storage onboard vehicles

Hydrogen is stored onboard the vehicles as a compressed gas for several reasons. First, high-pressure hydrogen storage tanks are a well-developed technology and the most prevalent method of hydrogen storage for HFCV prototypes. Second, compressed hydrogen storage requires significantly less energy to create it (10% of the LHV of the fuel) compared with cryogenic liquid hydrogen storage (requiring 30% of the LHV.) Also, compressed hydrogen storage requires

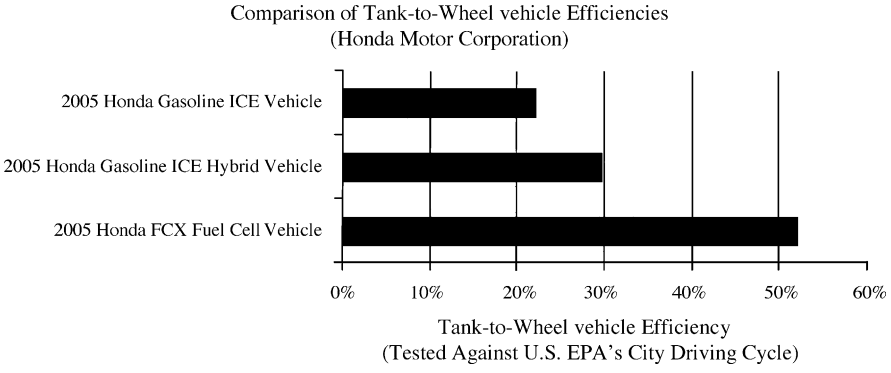

Fig. 7. Comparison of vehicle efficiencies for a new standard gasoline ICE vehicle, a new gasoline hybrid electric vehicle, and a new fuel cell vehicle, all built by Honda. Vehicles were tested by Honda against the U.S. EPA's City Driving Cycle, which characterizes the velocity profile of American cars driving through urban areas over time. Fuel cell vehicles have their maximum efficiency at lower powers, compared with gasoline ICE vehicles that have their efficiency sweet spot at higher powers. For this reason in part, the ratio of fuel cell vehicle efficiency to gasoline ICE efficiency is expected to be higher over urban driving cycles (lower average power) than highway driving cycles (higher average power). The ratio of efficiencies may be less for highway driving. Honda's 2005 FCX fuel cell vehicle uses an ultracapacitor to recapture breaking energy and to manage the electrical load by the motor.

Table 3
Volumetric and mass storage density estimates of three types of hydrogen storage systems: (1) compressed tanks, (2) cryogenic liquid tanks, and (3) metal hydrides, based on 2005 technology

Hydrogen storage system	Volumetric storage density (kg H_2 L^{-1})	Volumetric storage energy density ((kW h) L^{-1})	Gravimetric storage energy density ((kW h) kg^{-1})
Pressurized tanks (700 bar)	0.034	1.4	2
Cryogenic liquid tank (<22 K)	0.045	1.8	5.7
Metal hydride (low)	0.027	1	0.25
Metal hydride (high)	0.084	3.3	0.8

All of the ancillary components to the storage system, including the thermal management sub-systems, pipes, and valves are included in the estimates. The third and forth columns refer to the energy stored in the hydrogen fuel per liter and per unit mass of storage system including fuel, respectively.

approximately 10% of the energy as liquid hydrogen for reheating before entering the vehicle's fuel cell stack [53]. Third, advanced compressed hydrogen tanks currently can store hydrogen at 700 bar [54], where they can achieve volumetric storage densities of about 0.034 kg H_2 L^{-1}, and can thereby approach liquid hydrogen storage densities of 0.045 kg H_2 L^{-1}, as shown in Table 3 in the first column "Volumetric Storage Density." General Motors has developed such advanced high-pressure compressed gas tanks made of reinforced carbon fiber composite materials operating at 700 bar and demonstrated them in its 2005 Sequel fuel cell car [55]. Toyota also has demonstrated 700 bar high pressure tanks in mid-2005 that enable a cruising range of more than 500 km for its HFCV [56]. These storage densities are high enough to store enough mass to achieve a reasonable driving range. Fourth, to achieve comparable range with FFOV, a compressed storage tank with a larger volume can be integrated into a HFCV with better utilization of space onboard the vehicle through power train design and a higher packing factor through storage tank design [57]. Fifth, compressed hydrogen storage is less likely to leak or to release hydrogen into the atmosphere than liquid storage, which is estimated to leak at a rate of 0.20% [58], which requires periodic venting of boiled-off gases to prevent vapor pressure build-up in the tank (an additional loss), and which also leaks more hydrogen during refueling due to boil-off (a further loss). For liquid hydrogen tanks that have been in storage for several days without use and then begin venting, hydrogen release is estimated at 1.0% per day over the venting period [59]. Sixth, for the same quantity stored hydrogen, pressurized tanks weigh less and take up less volume compared with metal hydride storage, as shown in Table 3 in the third and forth columns labeled "Volumetric Storage Energy Density" and "Gravimetric Storage Energy Density." They also probably cost less [60]. Finally, future hydrogen storage technologies are projected to achieve higher storage densities with lower energy requirements, such that the assumption of compressed hydrogen tanks for a future fleet is reasonable.

The hydrogen compression energy (10^6 J $year^{-1}$) (ΔH_{H_2}) is

$$\Delta H_{H_2} = m_{H_2C} L_h \varphi_{H_2} \quad (3)$$

where φ_{H_2} is the hydrogen compression energy as a percentage of the LHV of the fuel, assumed here to be 0.10. [61] This value for φ_{H_2} assumes multi-stage compression, based on available compressor manufacturer's devices, to between 200 and 800 bar. This compression energy value lies between those for adiabatic and isothermal compression.

2.6.4. Hydrogen released via leakage or incomplete combustion in the supply chain

Hydrogen scenarios must incorporate the potential effects of hydrogen leakage because hydrogen (1) has a greater tendency to escape from confined spaces than do other gaseous fuels, (2) is likely to reside in the atmosphere for a long time after leakage, (3) may act to reduce the protective ozone layer in the upper atmosphere (stratosphere), (4) may increase the formation of the greenhouse gas methane, and (5) may increase harmful ozone in the lower atmosphere (troposphere). Hydrogen has a greater tendency to permeate small openings than other gaseous fuels do because it is one of the smallest molecules. Its diffusion coefficient in air is 0.61 cm^2 s^{-1} at room temperature, compared with 0.16 cm^2 s^{-1} for natural gas. When hydrogen leaks into air, it does not combust with oxygen in air in low concentrations at room temperature. Its ignition limits in air are between 4 and 75% by volume and its self-ignition temperature is 860 K. During leakage from high pressure storage tanks, hydrogen will disperse much faster than other fuels will due to its high sonic velocity, 1300 m s^{-1} compared with 450 m s^{-1} for natural gas. As a result, many hydrogen leakage events will not lead to high enough concentrations for combustion. Once escaped, hydrogen has a chemical lifetime in the atmosphere of 4.5–10 years, but an overall lifetime of 2–3 years due mostly to microbial uptake.

Hydrogen reacts with other molecules such that it may affect the stratospheric and tropospheric chemistry. It (1) may reduce the protective ozone layer in the stratosphere that shields the Earth from high levels of harmful ultraviolet radiation, (2) may increase methane, a greenhouse gas, and (3) may increase poisonous ozone, an air pollutant, in the troposphere. In the first case, it is hypothesized that hydrogen may reduce stratospheric ozone by increasing stratospheric water vapor, according to the reaction

$$H_2 + OH \rightarrow H_2O + H. \quad (R1)$$

An increase in stratospheric water vapor can increase the occurrence and size of Polar Stratospheric Clouds and

aerosols, on which reactions that destroy stratospheric ozone are initiated.

In the second case, it is hypothesized that hydrogen may increases methane, a greenhouse gas, in the troposphere. Hydrogen may react with OH by the reaction (1), such that the concentration of OH is reduced. The presence of OH might otherwise reduce the concentration of methane via the reaction

$$CH_4 + OH \rightarrow CH_3 + H_2O. \quad \text{(R2)}$$

In this way, an increased concentration of hydrogen in the troposphere may increase the concentration of methane.

In the third case, scientists have proposed that hydrogen may increase tropospheric ozone by reaction (1) that produces atomic hydrogen. Atomic hydrogen may in turn react to increase ozone, by these reactions,

$$H + O_2 + M \rightarrow HO_2 + M \quad \text{(R3)}$$

$$NO + HO_2 \rightarrow NO_2 + OH \quad \text{(R4)}$$

$$NO_2 + h\nu \rightarrow NO + O \quad \text{(R5)}$$

$$O + O_2 + M \rightarrow O_3 + M, \quad \text{(R6)}$$

where M is any air molecule that is neither created nor destroyed by the reaction and takes away the extra energy from the reaction, and $h\nu$ represents a photon. However, while all of these reactions above are valid, the overall conclusion that hydrogen will have these net effects is not yet proven, and may be unjustified. Converting from fossil fuels to hydrogen has many feedbacks to climate not previously simulated that may cause chemical reactions and produce feedbacks that could give the opposite conclusion. As a result, this study focuses on the net changes in all emissions, not just an increase in a single one.

For the HFCV scenarios, hydrogen may leak into the atmosphere at various points in the hydrogen supply chain. These include: (1) hydrogen production (Fig. 4, process 4), (2) hydrogen pipeline transmission and distribution (Fig. 4, process 5), (3) hydrogen compression (Fig. 4, process 6), (4) hydrogen storage (Fig. 4, process 7), (5) fuel dispensing, (6) fuel storage onboard vehicle, (7) fueling system onboard vehicle, and (8) fuel cell stack and system onboard vehicle. Of these, among the most crucial may be the last listed, hydrogen leakage onboard the vehicle at the fuel cell stack. Many fuel cell systems currently must vent hydrogen gas and water vapor at the anode to prevent liquid water from building up at reaction sites and blocking them. As a result, in many fuel cell system designs, hydrogen is periodically released from the stack. Another important source of hydrogen leakage is pipeline transmission and distribution. These primarily affect centralized production scenarios (coal) due to the longer distances hydrogen is conveyed over pipes. Leakage during distribution can be estimated by leakage at industrial hydrogen distribution facilities, one of which reports a leakage rate of only 0.10% [62]. Of the sources listed above, among the least crucial is hydrogen release due to storage tank failure (either on or off the vehicle). If a hydrogen tank fails via rupture or leakage, hydrogen is released. However, because tank failure is rare, hydrogen leakage associated with it is negligible. For example, since 1976, only 15 compressed natural gas (CNG) tanks have ruptured and only 20 have leaked for the 1 million CNG vehicles worldwide [63].

From the hydrogen consumption information, estimates of leakage hydrogen for the HFCV scenarios were derived. We consider an extreme case of 10% leakage of all hydrogen produced. Even considering all of the potential sources of leakage above, a 10% leakage rate is an unlikely overestimate of the hydrogen leakage in a future hydrogen economy based on gaseous hydrogen transport and storage. In a liquid-based hydrogen economy, hydrogen may leak when transported from the production site to the truck, from truck to the fuel station, and from fuel station to the vehicle, particularly if the lines are warm, such that the cold liquid hydrogen vaporizes. Such a liquid hydrogen economy could result in a significant leakage rate [64]. However, this liquid hydrogen economy is also impractical because it is highly energy intensive (30% of the LHV of the fuel is required for liquefaction, not including transport.) By contrast, in a gaseous-based hydrogen economy, assumed here, a reasonable estimate of hydrogen leakage may be between 1.0 and 3.0%. Natural gas leaks from new infrastructure in the U.S. at a rate of about 1.0% [65]. Because hydrogen is a smaller molecule than methane, it may diffuse more easily and may leak at a greater rate. Ultimately, this leakage rate will be determined by economics, and market forces are unlikely to support the production of a resource that is then lost at a rate of 10%.

Another reason for considering an extreme hydrogen leakage rate of 10% is that it introduces an additional element of conservatism with respect to energy consumption and emissions production along all points in the HFCV supply chains. With the 10% leakage assumption, energy requirements for producing hydrogen through electrolysis, steam reforming, or coal gasification will be over-estimates, as well as energy requirements for transport of fuel and related raw material resources. This further leads to conservative conclusions.

We consider an upper bound on hydrogen leakage for illustrative purposes to demonstrate conservative conclusions. In other words, if at such a high hydrogen leakage rate, the use of HFCV still reduces air pollution and greenhouse gases significantly, then at a lower leakage rate, the effects of HFCV can only be less damaging. Hydrogen emission via leakage (10^6 kg year^{-1}) was calculated according to

$$m_{H_2\_Leak} = m_{H_2P}\ell_{H_2} \quad (4)$$

where m_{H_2P} is the mass flow rate of hydrogen produced at the natural gas steam reformer, coal gasification plant, or electrolyzer and $m_{H_2\_Leak}$ is the mass flow rate of hydrogen leaked in between its production and its consumption by the HFCV. The total quantity of hydrogen emitted in a scenario is the sum of the quantity leaked and the quantity emitted during incomplete combustion, for example, at electric power plants [23].

2.6.5. Emission during the production of incremental electrical power

Emissions arise during the generation of electricity needed for hydrogen compression and production. In the model, this energy is provided by electricity from the 1999 mix of stationary power plants in the U.S., approximately 52% coal, 20% nuclear, 16% natural gas, 7.2% hydroelectric, 2.8% oil, 2.0% non-hydro renewable, and less than 1% other fossil fuels [66].

2.7. Scenario 2: hydrogen production via decentralized natural gas steam reforming

In this scenario, shown in Fig. 2, hydrogen is derived from natural gas, which is extracted from gas fields, stored, chemically processed, and transmitted through pipelines to distributed fuel processing units (following, up to this point, the same fuel cycle currently in place for gas turbine power plants and residential heating). The fuel processing units, situated in similar locations as gasoline refueling stations, convert natural gas to hydrogen via a combination of steam reforming and fuel oxidation [67,68]. Purified hydrogen is then compressed for use in HFCV.

This scenario assumes decentralized steam reformers are located close to the source of hydrogen demand at the vehicles. Compared with a centralized steam reformer scenario, a decentralized steam reformer scenario is more practical to achieve in the medium-term and has a lower marginal cost than a centralized one because: (1) it depends on the existing natural gas pipeline network rather than building a new network of hydrogen pipelines requiring expensive reinforced steels; (2) it can rely on economies of scale in mass production to bring down the manufacturing cost of the fuel reformers; (3) it can rely on existing refueling infrastructure with natural gas steam reformers located at similar locations as present-day gasoline or diesel refueling stations; and (4) it allows for incremental growth of a network of hydrogen refueling stations. This decentralized natural gas refueling infrastructure parallels that already intellectually established for stationary fuel cell systems converting natural gas to hydrogen with steam reformers and producing heat and power [69,70]. In the model, the steam reformers were located at similar locations to present-day refueling stations based on information in the NEI.

2.7.1. Emission during the production of hydrogen from natural gas

Decentralized steam reformers chemically convert natural gas into a hydrogen-rich gas. Emission from decentralized reformers were assumed to be those from United Technology Corporation's (UTC) PureCell steam reformer unit for its 200 kWe stationary hydrogen fuel cell system that produces electric power and heat. This commercial steam reformer's emission factors are shown in Table 4. They are based on Federal and California State environmental testing of the units, and are legally binding regarding their performance

Table 4
Natural gas steam reformer

Emission	Emission factor (kg of pollutant kg^{-1} of natural gas fuel)
NO_x	0.0000459
CO	0.00000328
NMHC	0.000000655
SO_x	Negligible
Particulates	Negligible
CH_4	0.0000475

[71]. Equating emissions from decentralized steam reformers with those from this commercial unit was a conservative assumption because more advanced steam reformer designs that incorporate more recent developments in catalysts and gas purification technologies could achieve lower emissions [72–74]. Carbon dioxide emissions were calculated based on the stoichiometric ratio of products to reactants in the chemical reactions involved. Energy needed for the endothermic steam reforming reaction was attained from the oxidation of methane.

For high efficiency steam reformers with low heat losses, the mass flow rate of natural gas (m_{NG}) needed to produce hydrogen for the vehicle fleet is

$$m_{NG} = \frac{m_{H_2C} M_{CH_4}}{M_{H_2}(1 + \phi_{M_{CH_4}})} \quad (5)$$

where M_{CH_4}/M_{H_2} is the ratio of the mass of methane consumed to the mass of hydrogen produced during the steam reforming and water gas shift reactions and $\phi_{M_{CH_4}}$ is the percentage of additional methane burned to provide heat to raise liquid water to steam for the steam reforming reaction (approximately 30%). Because the steam reforming reaction,

$$CH_4 + H_2O \rightarrow 3H_2 + CO, \quad (R7)$$

and the water gas shift reaction,

$$CO + H_2O \rightarrow H_2 + CO_2, \quad (R8)$$

exhibit fast reaction kinetics in the presence of commercial catalysts, it is reasonable to assume that the steam reforming reaction produces three moles of molecular hydrogen per mole of methane, and the water gas shift reaction produces one mole of hydrogen for each mole of carbon monoxide emanating from the steam reforming process. Combining these last two reactions gives the overall steam reforming reaction as

$$CH_4 + 2H_2O \rightarrow 4H_2 + CO_2, \quad (R9)$$

with a steam-to-carbon ratio of two. Although steam reforming reactors may operate with an excess of steam in the input to shift the equilibrium of the reaction towards hydrogen production (Le Chatlier's Principle), this excess steam in the input does not significantly affect the overall reaction above. Excess steam also does not affect the energy balance around the reactor because it is typically condensed at the outlet to

recapture the latent heat of vaporization. Under these assumptions, the mass ratio is two:

$$\frac{M_{CH_4}}{M_{H_2}} = 2. \quad (6)$$

We derive an emission factor for the fuel reformer of 2.65 kg CO_2 kg^{-1} of natural gas, which is consistent with UTC's estimate for their fuel reformer of 2.7 kg CO_2 kg^{-1} of natural gas [75].

Fuel reformers can achieve high efficiency and low heat losses through a variety of design options. These include insulation, capturing solar thermal energy to provide heat for the endothermic steam reforming or methane dissociation reactions [76–78], and reusing waste heat from other processes. Natural gas-to-hydrogen fuel reformers that incorporate either of the last of these two options can achieve an even higher efficiency, lower fuel consumption, and lower carbon dioxide emissions that the reformers assumed in this study.

2.7.2. Methane leakage

From the hydrogen consumption information, estimates of leaked methane were derived. Methane is the primary constituent in natural gas (typically 95% by volume), and also a greenhouse gas with a 100-year global warming potentially approximately 23 times that of carbon dioxide [79]. Within the current supply chain for natural gas used to heat buildings and provide fuel for power plants, the estimated methane leakage rate for new pipeline infrastructure is 1.0% of methane consumption [80]. This leakage rate refers to the leakage expected from the newest installations of gas transport and processing technologies in the U.S., i.e. the incremental rate, not the average rate from current infrastructure. We assume the same methane leakage rate for new infrastructure to support a natural gas HFCV supply chain.

2.8. Scenario 3: hydrogen production via decentralized wind electrolysis

In this scenario, shown in Fig. 3, hydrogen is derived from the electrolysis of water, powered by wind-generated electricity. The wind generated electricity is transmitted across the country to electrolyzers at distributed hydrogen refueling stations situated in the same locations as today's gasoline stations, according to NEI data. While electricity for the electrolysis of water for hydrogen production is attained from wind sources, electricity for compression of hydrogen is attained from the current mix of electric generation plants. Therefore, the main source of emission in this scenario is conventional power plants. Because the compression energy is approximately 5.0% of the energy required for electrolysis, the assumption of using conventional generation for compression power does not have a large impact on the analysis.

The number of wind turbines (n) to provide enough electricity for hydrogen production is estimated from

$$n = \frac{m_{H_2C} H_h}{E_T \eta_{AC} \eta_{LH} \eta_T \eta_D \eta_E}, \quad (7)$$

where m_{H_2C} is the total mass of hydrogen consumed by all vehicles in the U.S. per year (57 MT $year^{-1}$), H_h is the higher heating value of hydrogen (140 MJ kg^{-1}), E_T a single turbine's annual energy output, η_{AC} the efficiency of converting the turbine's variable AC power to constant frequency AC (∼97%), η_{LH} the efficiency of converting the turbine's low voltage electricity up to high voltage electricity for conveying across long distances (∼95%), η_T the high voltage transmission grid efficiency that includes losses due to resistance in the wires (∼97%),[81] η_D the low voltage transmission grid efficiency including wire resistance (∼93%) [81], and η_E the electrolyzer efficiency (∼73%) [82]. E_T can be estimated from

$$E_T = 8760 P_r \left(0.087\,V - \frac{P}{D^2}\right) \quad (8)$$

where E_T is in (kW h) $year^{-1}$, 8760 is the number of hours in a year, P_r the rated power of the turbine (kW), V the mean annual Rayleigh distributed wind speed (m s^{-1}) at turbine hub height, and D the diameter (m) of the turbine [83,84]. General Electric produces a 3.6 MW turbine with a 104 m blade [85]. In the presence of 7.75 m s^{-1} winds, the turbine energy produced is estimated to be 10.8 million (kW h) $year^{-1}$. The total number of turbines needed is about 340,000. The land area required for each wind turbines is the product of 4D and 7D [84]. For the GE turbine, each turbine requires a land area of 0.30 km^2. The total area for these turbines to minimize interference is about 100,000 km^2, the approximate land area of the state of Pennsylvania, which could be spread over land or ocean.

2.9. Scenario 4: hydrogen production via centralized coal gasification

In this scenario, shown in Fig. 4, hydrogen is derived from coal, which is extracted from mines and chemically processed into a hydrogen rich gas at centralized coal gasification plants. Carbon dioxide released at coal plants is not sequestered, although the gasification plant technology assumed here would allow this. (Carbon sequestration refers to the long-term storage of carbon in the ground in geological repositories, the oceans, or the biological surroundings such that carbon dioxide, the primary greenhouse gas, builds up in concentration in the atmosphere at a lower rate.) In the model, the coal gasification plants are situated in the same locations as conventional coal combustion plants for electricity production are situated today, according to NEI data. Hydrogen is then transmitted through pipelines to refueling stations.

2.9.1. Coal gasification process

Coal gasification for hydrogen production is a process of chemically and thermally converting solid coal into a gaseous mixture of primarily hydrogen, carbon monoxide, and other hydrocarbons such as methane. The gasifier converts coal into primarily H_2 and CO in the presence of steam at high temperature and pressure. For comparison, in a combustion process, the stoichiometric amount of oxygen is supplied such that the fuel can be completely oxidized to the full products of combustion (CO_2 and H_2O). By contrast, in a gasification process, a much smaller quantity of oxygen is delivered to the fuel, at a higher temperature and pressure, such that the fuel can not completely combust and rather "partially oxidizes" to the incomplete combustion products of CO and H_2. The exothermic partial oxidation of the fuel provides heat. The "incomplete combustion products" from gasification, CO and H_2, are referred to as syngas [86]. As with natural gas steam reforming discussed above, the water gas shift reaction is used to shift CO in the presence of steam to additional H_2.

Because coal is a hydrogen-deficient fuel, it must be combined with water or another source of hydrogen to be used as a fuel in hydrogen production. Coal has less hydrogen per mole of carbon than do most other hydrocarbon fuels (a hydrogen-to-carbon ratio near 0.80), as compared with liquid hydrocarbons with a ratio near 2 (such as gasoline and diesel) and gaseous hydrocarbons with a ratio near 4 (such as natural gas). For this reason, coal, when used as a feedstock in hydrogen production, must be combined with another hydrogen source such as water. As a result, the quantity of greenhouse gas emissions (especially CO_2) and air pollutants emitted from a coal gasification plant is highly dependent on the steam to carbon ratio that the plant is assumed to operate at. At the same time, the more water added to the process for hydrogen production, the more energy needed to raise the steam and to break the hydrogen bonds. This energy is provided by the coal fuel, such that there is a maximum quantity of hydrogen that can be produced from a given amount of coal fuel input, assuming no additional source of thermal energy.

No advanced coal gasification plants maximized for hydrogen production have been built to date in the U.S. As a result, emission measurements or energy usage data from such a plant are not available. Consequently, the emission and energy requirements for the plant in this model are based on a DOE study examining the reconfiguration of a coal gasification plant from electricity production to hydrogen production [87]. Emissions and energy use requirements are based on this chemical engineering simulation study.

Unlike the natural gas steam reformers assumed in this study, the coal gasification plant designs assumed in this study require a net electric power input from the grid. These gasification plants are maximized for hydrogen production and therefore follow a different design, with different emission profiles, than prototype gasification plants built in the U.S. for electricity production. These gasification plants for hydrogen production are assumed not to use downstream gas turbines, but rather steam turbines for electric generation. They also require additional electric power input from the grid.

2.9.2. Coal consumption at gasification plant

The quantity of coal consumed at the gasification plant is estimated from the hydrogen consumption requirements for the vehicles. The mass flow rate of dry coal ($m_{\mathrm{COAL\,C}}$) consumed at the centralized gasification plants for production of hydrogen for the vehicle fleet is

$$m_{\mathrm{COAL\_C}} = \frac{m_{\mathrm{H_2C}}\, M_{\mathrm{Coal}}}{M_{\mathrm{H_2}}}, \tag{9}$$

where $M_{\mathrm{Coal}}/M_{\mathrm{H_2}}$ is the ratio of the mass of coal consumed to the mass of hydrogen produced during coal gasification, estimated here as 7.6. The mass of wet coal delivered to the coal plant per county per year (10^6 kg year^{-1}) is described according to

$$m_{\mathrm{COAL\_D}} = \frac{m_{\mathrm{COAL\_C}}}{(1-\psi_{\mathrm{COAL}})} \tag{10}$$

where $m_{\mathrm{COAL\,D}}$ is the mass flow rate of wet coal delivered to coal plant (10^6 kg year^{-1}), $m_{\mathrm{COAL\,C}}$ the mass flow rate of dry coal consumed in gasification plant (10^6 kg year^{-1}), and ψ_{COAL} the moisture content of wet coal = 0.15.

2.9.3. Coal gasification plant emissions

Coal gasification plant emissions are based on coal consumption requirements. Table 5 shows the relevant emission factors. Carbon dioxide emissions (10^6 kg year^{-1}) ($m_{\mathrm{CO_2}}$) are quantified according to

$$m_{\mathrm{CO_2}} = 2.37\, m_{\mathrm{COAL\_C}}. \tag{11}$$

NO_2 emissions (10^6 kg year^{-1}) ($m_{\mathrm{NO_2}}$) are calculated according to

$$m_{\mathrm{NO_2}} = m_{\mathrm{COAL\_C}} \gamma_{\mathrm{NO_2}}, \tag{12}$$

where $\gamma_{\mathrm{NO_2}}$ is the emission factor for NO_2 emanating from the gasification plant per unit of coal fuel consumed. Emission of CO, VOC, SO_2, and particles are calculated similarly using the emission factors in Table 5.

2.9.4. Coal gasification plant energy use

According to the DOE's coal gasification plant design, the plant must consume additional electric power for gasification. The additional electric power required for running

Table 5
Coal gasification plant

Emission	Emission factor (kg of pollutant kg^{-1} of dry coal fuel)
SO_x as SO_2	0.000762
NO_x as NO_2	0.000108
CO	0.00734
VOC	0
Particulates	0
CO_2	2.37

the gasification plant per county per year (10^6 kg year^{-1}) ($\Delta H_{\text{GASIFICATION}}$) is calculated as

$$\Delta H_{\text{GASIFICATION}} = m_{\text{COAL\_C}} h_{\text{GASIFICATION}}, \quad (13)$$

where $h_{\text{GASIFICATION}}$ is the additional electric power required per unit of coal fuel consumed, 580,000 MJ/10^6 kg coal consumed.

3. Results

3.1. Gaseous and particle emissions for each scenario by category

Tables 6 through 9 show gas and particle emissions from all anthropogenic sources from each of the four scenarios broken down into three main categories: (1) on-road vehicles and upstream hydrogen supply chain, (2) non-road mobile sources, and (3) point and area sources, which include electric power plants. Although the second category is constant across scenarios, the first and third categories vary. HFCV emit only water vapor and leaked hydrogen. However, the on-road vehicles category includes upstream emission in the hydrogen supply chain. These include steam reforming emission (CO, NO_x, HCHO, CH_4, CO_2), coal gasification emission (CO, NO_x, SO_x, CO_2), H_2 leakage, and, in the natural gas case, CH_4 leakage.

These tables also list H_2, CO_2, and H_2O emission under slightly different source categories: (1) on-road vehicles and upstream hydrogen supply chain, (2) other sources, and (3) electric power plants. For example, in the natural gas and coal HFCV scenarios, CO_2 emission listed under the "on-road vehicles" category refers to emissions from the steam reformers and the coal gasification plants, respectively. Emissions due to electric power generation required for hydrogen

Table 6
Hybrid electric vehicle scenario emission production (metric ton year^{-1})

Species	On-road vehicles	Non-road mobile sources	Point and area sources including electric power plants	Total
Gases				
Carbon monoxide (CO)	4.27E+07	2.28E+07	2.71 E+07	9.26E+07
Nitrogen oxides (NO_x) as NO_2	5.22E+06	4.02E+06	1.03E+07	1.96E+07
Organics				
Paraffins (PAR)	2.43E+06	1.74E+06	8.75E+06	1.29E+07
Olefins (OLE)	1.11E+05	8.53E+04	2.75E+05	4.71 E+05
Ethylene (C_2H_4)	1.57E+05	1.27E+05	5.58E+05	8.42E+05
Formaldehyde (HCHO)	3.06E+04	4.91 E+04	1.29E+05	2.09E+05
Higher aldehydes (ALD2)	1.19E+05	9.36E+04	7.34E+04	2.86E+05
Toluene (TOL)	2.27E+05	1.63E+05	2.11E+06	2.50E+06
Xylene (XYL)	3.21 E+05	2.19E+05	1.56E+06	2.10E+06
Isoprene (ISOP)	3.35E+03	2.05E+03	3.01 E+03	8.41 E+03
Total non-methane organics	3.40E+06	2.48E+06	1.35E+07	1.93E+07
Methane (CH_4)	5.46E+05	4.24E+05	5.10E+06	6.07E+06
Sulfur oxides (SO_x) as SO_2	1.88E+05	4.29E+05	1.74E+07	1.80E+07
Ammonia (NH_3)	1.65E+05	3.25E+04	4.26E+06	4.46E+06
Hydrogen (H_2)	1.22E+06	6.49E+05	7.74E+05	2.64E+06
Particulate matter				
Organic matter ($OM_{2.5}$)	3.48E+04	8.89E+04	2.50E+06	2.62E+06
Black carbon ($BC_{2.5}$)	6.26E+04	1.32E+05	3.69E+05	5.64E+05
Sulfate ($SULF_{2.5}$)	1.30E+03	6.12E+03	3.02E+05	3.09E+05
Nitrate ($NIT_{2.5}$)	1.70E+02	7.05E+02	2.58E+04	2.66E+04
Other ($OTH_{2.5}$)	1.66E+04	6.16E+04	8.17E+06	8.25E+06
Total $PM_{2.5}$	1.15E+05	2.89E+05	1.14E+07	1.18E+07
Organic matter (OM_{10})	4.96E+04	9.71 E+04	5.60E+06	5.74E+06
Black carbon (BC_{10})	7.38E+04	1.44E+05	7.10E+05	9.28E+05
Sulfate ($SULF_{10}$)	2.06E+03	6.69E+03	4.82E+05	4.90E+05
Nitrate (NIT_{10})	2.17E+02	7.72E+02	6.99E+04	7.09E+04
Other (OTH_{10})	2.53E+04	6.72E+04	3.74E+07	3.75E+07
Total PM_{10}	1.51 E+05	3.16E+05	4.43E+07	4.48E+07
Species	On-road vehicles	Other sources	Electric power plants	Total
Carbon dioxide (CO_2)	1.06E+09	1.70E+09	2.23E+09	4.98E+09
Water (H_2O)	3.99E+08	6.38E+08	8.38E+08	1.87E+09
CO_2 equivalent (low)	1.05E+09	1.70E+09	2.27E+09	5.02E+09
CO_2 equivalent (high)	1.07E+09	1.74E+09	2.72E+09	5.53E+09

Table 7
Natural gas hydrogen fuel cell vehicle (HFCV) scenario emission production (metric ton year^{-1})

Species	On-road vehicles and upstream H_2 supply chain	Non-road mobile sources	Point and area sources including electric power plants	Total
Gases				
Carbon monoxide (CO)	5.35E+02	2.28E+07	2.72E+07	4.99E+07
Nitrogen oxides (NO_x) as NO_2	7.49E+03	4.02E+06	1.06E+07	1.46E+07
Organics				
Paraffins (PAR)	0.00E+00	1.74E+06	8.48E+06	1.02E+07
Olefins (OLE)	0.00E+00	8.54E+04	2.67E+05	3.52E+05
Ethylene (C_2H_4)	0.00E+00	1.27E+05	5.58E+05	6.85E+05
Formaldehyde (HCHO)	1.07E+02	4.91E+04	1.30E+05	1.79E+05
Higher aldehydes (ALD2)	0.00E+00	9.36E+04	6.91 E+04	1.63E+05
Toluene (TOL)	0.00E+00	1.63E+05	2.01 E+06	2.17E+06
Xylene (XYL)	0.00E+00	2.18E+05	1.41 E+06	1.62E+06
Isoprene (ISOP)	0.00E+00	2.06E+03	2.95E+03	5.01 E+03
Total non-methane organics	1.07E+02	2.48E+06	1.29E+07	1.54E+07
Methane (CH_4)	2.12E+06	4.25E+05	5.08E+06	7.63E+06
Sulfur oxides (SO_x) as SO_2	0.00E+00	4.29E+05	1.80E+07	1.85E+07
Ammonia (NH_3)	0.00E+00	3.24E+04	4.26E+06	4.29E+06
Hydrogen (H_2)	6.31 E+06	6.49E+05	7.74E+05	7.74E+06
Particulate matter				
Organic matter ($OM_{2.5}$)	0.00E+00	8.89E+04	2.50E+06	2.59E+06
Black carbon ($BC_{2.5}$)	0.00E+00	1.32E+05	3.70E+05	5.03E+05
Sulfate ($SULF_{2.5}$)	0.00E+00	6.15E+03	3.03E+05	3.09E+05
Nitrate ($NIT_{2.5}$)	0.00E+00	7.02E+02	2.58E+04	2.65E+04
Other ($OTH_{2.5}$)	0.00E+00	6.13E+04	8.18E+06	8.24E+06
Total $PM_{2.5}$	0.00E+00	2.89E+05	1.14E+07	1.17E+07
Organic matter (OM_{10})	0.00E+00	9.67E+04	5.60E+06	5.70E+06
Black carbon (BC_{10})	0.00E+00	1.44E+05	7.13E+05	8.57E+05
Sulfate ($SULF_{10}$)	0.00E+00	6.70E+03	4.83E+05	4.90E+05
Nitrate (NIT_{10})	0.00E+00	7.76E+02	7.00E+04	7.08E+04
Other (OTH_{10})	0.00E+00	6.40E+04	3.75E+07	3.75E+07
Total PM_{10}	0.00E+00	3.12E+05	4.43E+07	4.46E+07
Species	On-road vehicles and upstream H_2 supply chain	Other sources	Electric power plants	Total
Carbon dioxide (CO_2)	4.49E+08	1.70E+09	2.36E+09	4.50E+09
Water (H_2O)	5.11E+08	6.38E+08	8.85E+08	2.03E+09
CO_2 equivalent (low)	4.98E+08	1.70E+09	2.39E+09	4.58E+09
CO_2 equivalent (high)	4.98E+08	1.74E+09	2.85E+09	5.08E+09

compression and coal gasification plant operation are included in the electric power plants category, which also includes emission from electric power for other purposes in the economy. The tables list H_2O emission for all HFCV scenarios of about 510 megatonnes (MT) H_2O year^{-1}, based on the uniform hydrogen consumption in all vehicles of 57 MT year^{-1} H_2 after leakage. The water vapor produced in the HFCV scenarios is the same for all three cases for the vehicles and upstream hydrogen supply chain. The steam reforming and coal gasification processes consume rather than produce water. In the coal HFCV case, additional water is produced by combustion at electric power plants for the additional electricity needed to run the coal gasification plants.

3.2. Net change in gaseous and particle emissions

Table 10 shows the net change in emission for each scenario compared with the base case of the 1999 vehicle fleet. In all HFCV scenarios, gas and particle emissions decreased significantly. The reduction in gas emission is similar for all HFCV scenarios, regardless of the method of producing hydrogen, due primarily to the elimination of FFOV emission. The reduction in particle emission is also similar for all HFCV scenarios. Hybrid emission reductions are only slightly less than the base case for most pollutants.

For the four scenarios, particle emission decreased significantly more in terms of number concentration than mass. Table 10 shows a relatively small reduction in particle mass because most particle mass was emitted by sources not affected by the LCA. These include electric power plants, boilers, furnaces, process plants, road dust, and agricultural dust. The reductions shown in Table 10, while not significant in terms of particle mass, are significant in terms of the particle number concentration and human health [88]. The particles that were removed from the four scenarios were primarily FFOV particles, which tend to be small. Small

Table 8
Wind electrolysis hydrogen fuel cell vehicle (HFCV) scenario emission production (metric ton year^{-1})

Species	On-road vehicles and upstream H_2 supply chain	Non-road mobile sources	Point and area sources including electric power plants	Total
Gases				
Carbon monoxide (CO)	0.00E+00	2.28E+07	2.72E+07	4.99E+07
Nitrogen oxides (NO_x) as NO_2	0.00E+00	4.02E+06	1.06E+07	1.46E+07
Organics				
Paraffins (PAR)	0.00E+00	1.74E+06	8.48E+06	1.02E+07
Olefins (OLE)	0.00E+00	8.54E+04	2.67E+05	3.52E+05
Ethylene (C_2H_4)	0.00E+00	1.27E+05	5.58E+05	6.85E+05
Formaldehyde (HCHO)	0.00E+00	4.91 E+04	1.30E+05	1.79E+05
Higher aldehydes (ALD2)	0.00E+00	9.36E+04	6.91 E+04	1.63E+05
Toluene (TOL)	0.00E+00	1.63E+05	2.01 E+06	2.17E+06
Xylene (XYL)	0.00E+00	2.18E+05	1.41 E+06	1.62E+06
Isoprene (ISOP)	0.00E+00	2.06E+03	2.95E+03	5.01E+03
Total non-methane organics	0.00E+00	2.48E+06	1.29E+07	1.54E+07
Methane (CH_4)	0.00E+00	4.24E+05	5.08E+06	5.51 E+06
Sulfur oxides (SO_x) as SO_2	0.00E+00	4.29E+05	1.80E+07	1.85E+07
Ammonia (NH_3)	0.00E+00	3.24E+04	4.26E+06	4.29E+06
Hydrogen (H_2)	6.31 E+06	6.49E+05	7.74E+05	7.74E+06
Particulate matter				
Organic matter ($OM_{2.5}$)	0.00E+00	8.89E+04	2.50E+06	2.59E+06
Black carbon ($BC_{2.5}$)	0.00E+00	1.32E+05	3.70E+05	5.03E+05
Sulfate ($SULF_{2.5}$)	0.00E+00	6.15E+03	3.03E+05	3.09E+05
Nitrate ($NIT_{2.5}$)	0.00E+00	7.02E+02	2.58E+04	2.65E+04
Other ($OTH_{2.5}$)	0.00E+00	6.13E+04	8.18E+06	8.24E+06
Total $PM_{2.5}$	0.00E+00	2.89E+05	1.14E+07	1.17E+07
Organic matter (OM_{10})	0.00E+00	9.67E+04	5.60E+06	5.70E+06
Black carbon (BC_{10})	0.00E+00	1.44E+05	7.13E+05	8.57E+05
Sulfate ($SULF_{10}$)	0.00E+00	6.70E+03	4.83E+05	4.90E+05
Nitrate (NIT_{10})	0.00E+00	7.76E+02	7.00E+04	7.08E+04
Other (OTH_{10})	0.00E+00	6.40E+04	3.75E+07	3.75E+07
Total PM_{10}	0.00E+00	3.12E+05	4.43E+07	4.46E+07
Species	On-road vehicles and upstream H_2 supply chain	Other sources	Electric power plants	Total
Carbon dioxide (CO_2)	0.00E+00	1.70E+09	2.36E+09	4.05E+09
Water (H_2O)	5.11E+08	6.38E+08	8.85E+08	2.03E+09
CO_2 equivalent (low)	0.00E+00	1.70E+09	2.39E+09	4.09E+09
CO_2 equivalent (high)	0.00E+00	1.74E+09	2.85E+09	4.58E+09

particles cause greater damage to human health (per unit mass of emission) than do large particles, because small particles permeate human tissue (such as the lungs) more readily [89]. Also, due to the close proximity between people and vehicles, more people are exposed to vehicle exhaust than to, for example, power plant exhaust. Thus, although the HFCV scenarios did not remove much particle mass, they removed a significant particle number concentration having a potentially large impact on health.

3.3. Net change in emissions for HFCV in comparison with hybrids

Regardless of the source of fuel, HFCV reduce almost all air pollutant and greenhouse gas emissions to a greater extent than do hybrids, as shown in Table 10. The only exceptions to this include: (1) SO_x, H_2, water vapor in all HFCV scenarios, (2) CH_4 in the natural gas HFCV scenario, and (3) CO_2 in the coal-HFCV scenario. These values are shown as positive in the HFCV cases in Table 10 (except for CO_2). With respect to (1), SO_x increases by about 2.0% in the wind and natural gas-HFCV scenarios as a result of the increased electrical power needed for hydrogen compression, supplied by the current power plant generation mix (52% coal). In the coal-HFCV scenario, SO_x increases even further to 5.4% due to: (1) the additional electric power needed to run the coal gasification plant and (2) the coal gasification process itself which emits SO_x. Also with respect to (1), H_2 emission increases with respect to hybrids because the assumed H_2 leakage rate of 10% in the HFCV scenarios results in a 143% increase in H_2. By contrast, H_2 emitted in the hybrid case decreases due to greater fuel economy and consequently less incomplete combustion at the vehicle. Additionally, with respect to (1), in all HFCV scenarios, water vapor emission increase slightly by between 2 and 3%. Water vapor emission is higher in the HFCV scenarios primarily due to a relative increase in

Table 9
Coal gasification hydrogen fuel cell vehicle (HFCV) scenario emission production (metric ton year^{-1})

Species	On-road vehicles and upstream H_2 supply chain	Non-road mobile sources	Point and area sources including electric power plants	Total
Gases				
Carbon monoxide (CO)	3.52E+06	2.28E+07	2.72E+07	5.35E+07
Nitrogen oxides (NO_x) as NO_2	5.18E+04	4.02E+06	1.07E+07	1.48E+07
Organics				
Paraffins (PAR)	0.00E+00	1.74E+06	8.48E+06	1.02E+07
Olefins (OLE)	0.00E+00	8.54E+04	2.67E+05	3.52E+05
Ethylene (C_2H_4)	0.00E+00	1.27E+05	5.58E+05	6.86E+05
Formaldehyde (HCHO)	0.00E+00	4.91 E+04	1.30E+05	1.79E+05
Higher aldehydes (ALD2)	0.00E+00	9.36E+04	6.91E+04	1.63E+05
Toluene (TOL)	0.00E+00	1.64E+05	2.01E+06	2.17E+06
Xylene (XYL)	0.00E+00	2.18E+05	1.41 E+06	1.62E+06
Isoprene (ISOP)	0.00E+00	2.06E+03	2.95E+03	5.01 E+03
Total non-methane organics	0.00E+00	2.48E+06	1.29E+07	1.54E+07
Methane (CH_4)	0.00E+00	4.24E+05	5.08E+06	5.51 E+06
Sulfur oxides (SO_x) as SO_2	3.65E+05	4.22E+05	1.83E+07	1.91E+07
Ammonia (NH_3)	0.00E+00	3.21 E+04	4.26E+06	4.29E+06
Hydrogen (H_2)	6.41 E+06	6.49E+05	7.75E+05	7.84E+06
Particulate matter				
Organic matter ($OM_{2.5}$)	0.00E+00	8.88E+04	2.50E+06	2.59E+06
Black carbon ($BC_{2.5}$)	0.00E+00	1.32E+05	3.71 E+05	5.03E+05
Sulfate ($SULF_{2.5}$)	0.00E+00	6.11E+03	3.03E+05	3.09E+05
Nitrate ($NIT_{2.5}$)	0.00E+00	7.00E+02	2.58E+04	2.65E+04
Other ($OTH_{2.5}$)	0.00E+00	6.16E+04	8.19E+06	8.25E+06
Total $PM_{2.5}$	0.00E+00	2.89E+05	1.14E+07	1.17E+07
Organic matter (OM_{10})	0.00E+00	9.69E+04	5.60E+06	5.70E+06
Black carbon (BC_{10})	0.00E+00	1.44E+05	7.14E+05	8.58E+05
Sulfate ($SULF_{10}$)	0.00E+00	6.80E+03	4.83E+05	4.90E+05
Nitrate (NIT_{10})	0.00E+00	7.70E+02	7.00E+04	7.08E+04
Other (OTH_{10})	0.00E+00	6.47E+04	3.75E+07	3.75E+07
Total PM_{10}	0.00E+00	3.13E+05	4.43E+07	4.46E+07
Species	On-road vehicles and upstream H_2 supply chain	Other sources	Electric power plants	Total
Carbon dioxide (CO_2)	1.14E+09	1.70E+09	2.40E+09	5.24E+09
Water (H_2O)	5.11E+08	6.38E+08	9.02E+08	2.05E+09
CO_2 equivalent (low)	1.13E+09	1.70E+09	2.43E+09	5.26E+09
CO_2 equivalent (high)	1.13E+09	1.74E+09	2.89E+09	5.76E+09

combustion products at electric power plants. By contrast, the hybrid scenario emits less water vapor due to a relative decrease in fuel consumption and products at the vehicle. With respect to (2), CH_4 emission increases in the natural gas HFCV scenario by 21% due to the assumed methane leakage rate of 1.0% of consumption in the upstream hydrogen fuel supply chain. CH_4 increased by 1.3 MT year^{-1}. With respect to (3), CO_2 emissions are slightly higher in the coal-HFCV scenario than in the hybrid scenario due to an increase in CO_2 emissions at the coal gasification plant that comes close to offsetting the decrease in CO_2 emissions at the vehicle.

Except for these specific cases, HFCV reduce all air pollutant and greenhouse gas emissions to a greater extent than do hybrids, even if fueled by fossil fuels such as natural gas and coal. A 2004 editorial article in a prestigious science journal suggested that, "[A]s long as hydrogen for fuel cell cars is provided from fossil fuels, much the same environmental benefits can be gained by adopting hybrid gasoline-electric and advanced diesel engines." [10] This analysis and the results presented in Table 10 suggest that environmental benefits with respect to air pollution and greenhouse gases could be more significant for HFCV than hybrid ICEs, as a result of the elimination of incomplete combustion products at the vehicle and the higher efficiency of the fuel cells compared with engines. Also, according to another 2004 article in the same journal, "[Hydrogen vehicles fueled by hydrogen produced from natural gas via steam reforming] represents only a modest reduction in vehicle emissions as compared to emissions from current hybrid vehicles." [90] The results presented in Table 10 suggest a significant reduction in well-to-wheels emissions for a natural gas-HFCV scenario compared with a hybrid one.

3.4. Net change in hydrogen emissions

Hydrogen emission increased significantly in all HFCV scenarios, compared with the base case of the current

Table 10
Percentage change from the 1999 conventional vehicle fleet change in emission production from the 1999 FFOV base case as a function of all anthroprogenic (man-made) sources

Species	Hybrid electric internal combustion engine (%)	HFCV and natural gas (%)	HFCV and wind electrolysis (%)	HFCV and coal gasification (%)
Gases				
Carbon monoxide (CO)	−17.14	−55.29	−55.30	−52.13
Nitrogen oxides (NO_x) as NO_2	−10.73	−33.18	−33.23	−32.50
Organics				
Paraffins (PAR)	−7.81	−27.10	−27.10	−27.10
Olefins (OLE)	−9.57	−32.43	−32.43	−32.43
Ethylene (C_2H_4)	−7.72	−24.86	−24.86	−24.85
Formaldehyde (HCHO)	−6.18	−19.68	−19.72	−19.63
Higher aldehydes (ALD2)	−15.73	−51.98	−51.98	−51.98
Toluene (TOL)	−3.92	−16.71	−16.71	−16.67
Xylene (XYL)	−6.44	−27.69	−27.69	−27.69
Isoprene (ISOP)	−15.20	−49.54	−49.54	−49.54
Total non-methane organics	−7.33	−26.24	−26.24	−26.24
Methane (CH_4)	−3.89	20.88	−12.75	−12.74
Sulfur oxides (SO_x) as SO_2	−0.48	2.05	2.05	5.37
Ammonia (NH_3)	−1.63	−5.25	−5.25	−5.25
Hydrogen (H_2)	−17.14	142.98	142.98	146.14
Particulate matter				
Organic matter ($OM_{2.5}$)	−0.59	−1.78	−1.78	−1.75
Black carbon ($BC_{2.5}$)	−4.76	−15.08	−15.08	−14.99
Sulfate ($SULF_{2.5}$)	−0.21	−0.32	−0.32	−0.23
Nitrate ($NIT_{2.5}$)	−0.29	−0.82	−0.82	−0.79
Other ($OTH_{2.5}$)	−0.09	−0.15	−0.15	−0.08
Total $PM_{2.5}$	−0.44	−1.26	−1.26	−1.21
Organic matter (OM_{10})	−0.39	−1.18	−1.18	−1.14
Black carbon (BC_{10})	−3.45	−10.87	−10.87	−10.77
Sulfate ($SULF_{10}$)	−0.19	−0.35	−0.35	−0.24
Nitrate (NIT_{10})	−0.14	−0.38	−0.38	−0.37
Other (OTH_{10})	−0.02	−0.03	−0.03	0.00
Total PM_{10}	−0.15	−0.41	−0.41	−0.38
Species				
Carbon dioxide (CO_2)	−5.96	−15.03	−23.50	−1.19
Water (H_2O)	−6.00	1.97	1.97	2.85
CO_2 equivalent (low)	−5.86	−14.00	−23.33	−1.33
CO_2 equivalent (high)	−5.52	−13.25	−21.75	−1.64

CO_2 equivalent refers to the weighted sum of the mass of CO_2 and CH_4 gases, where CH_4 is weighted by its global warming potential relative to CO_2. Over a 100-year period, CH_4 is estimated to have a global warming effect on the climate 23 times greater than that of CO_2.

vehicle fleet, with the assumption of 10% hydrogen leakage – an upper bound for the leakage rate. Based on uniform hydrogen production of 63 MT H_2 $year^{-1}$ before leakage, a 10% leakage rate results in total of 6.3 MT H_2 $year^{-1}$ leaked, as shown in Tables 7 through 9. In practice, the natural gas and wind scenarios would probably emit less hydrogen than the coal scenario, because the decentralized production of hydrogen by natural gas steam reformers and electrolyzers results in significantly less hydrogen transmission and distribution piping infrastructure, and leakage is partly a function of gas transmission distance.

Hydrogen was emitted in the base case via incomplete combustion at: (1) vehicles and (2) electric power plants. Because CO and H_2 are both products of incomplete combustion, the quantity of H_2 emitted from the 1999 conventional vehicle fleet was derived from the quantity of CO emission recorded in the NEI. Based on a CO emission of 62 MT CO $year^{-1}$ and 0.0285 units of mass of H_2 per unit of mass of CO for combustion processes [23], the base case conventional fleet emitted 1.8 MT H_2 $year^{-1}$. This corresponds to a hydrogen leakage rate from a HFCV scenario of approximately 3%. Also a result of incomplete combustion, on-road mobile sources and point and area sources including electric power plants also emitted H_2 as a result of incomplete combustion, equivalent to a hydrogen leakage rate of approximately 2%. Therefore, at more realistic hydrogen leakage rates (<3%), a HFCV fleet would leak less hydrogen than the current vehicle fleet emits due to incomplete combustion.

The hybrid scenario resulted in reduced H_2 since H_2 is a fossil-fuel combustion product, so reducing fossil-fuel emissions reduced H_2 emission.

3.5. Net change in water vapor emissions

As shown in Table 10, total water vapor emission decreased slightly in the hybrid case (by 6%) and increased slightly in all HFCV scenarios (by 2–3%). In all scenarios (hybrid and HFCV), water vapor emission decreased at the vehicles compared with the base case. However, in the HFCV scenarios, the total water vapor emission increased across the entire supply chain due to an increase in consumption of electrical power for hydrogen compression and production. These conventional fossil-fuel electric plants produced water as a product of combustion.

At the vehicle, emission of water vapor decreased slightly for all HFCV scenarios, as shown by conservation of mass calculations. According to assumptions of this analysis regarding the relative efficiency of FFOV and HFCV, a 1999 FFOV fleet that consumes approximately 450 MT year^{-1} gasoline and diesel fuel would equate to a HFCV fleet that consumes about 57 MT year^{-1} hydrogen fuel, as discussed in Section 2.6.2, "Hydrogen Consumption by Vehicles."

Within a fuel cell, each mole of hydrogen (2 g H_2) consumed produces one mole of water vapor (18 g H_2O), by the reaction

$$H_2 + 0.5O_2 \rightarrow H_2O + \text{electricity} + \text{heat}. \quad \text{(R10)}$$

Given a ratio of 9 kg of H_2O kg^{-1} of H_2, 57 MT year^{-1} H_2 consumed at the HFCV produces about 510 MT year^{-1} H_2O.

By contrast, combustion of vehicle fuel can be approximated by stoichimetric combustion. Gasoline ($C_nH_{1.87n}$) and light diesel ($C_nH_{1.8n}$) [35] fuels represent 78 and 22% of 1999 fuel consumption in vehicles [91], respectively. A molar mixture of the two fuels weighted by their relative consumption in vehicles is $CH_{1.85}$. Stoichiometric combustion of $CH_{1.85}$ described by,

$$CH_{1.85} + 1.4625O_2 \rightarrow CO_2 + 0.925H_2O + \text{heat}, \quad \text{(R11)}$$

such that one mole of fuel (14 g of $CH_{1.85}$) consumed produces one mole of CO_2 (44 g of CO_2) and 0.93 mole of water vapor (17 g of H_2O). Thus, for every 450 MT year^{-1} fuel consumed in FFOV, approximately 540 MT H_2O year^{-1} is produced. Another estimation method can be based on the ratio of emitted water to emitted CO_2. (0.38 kg of H_2O kg^{-1} of CO_2) and the quantity of CO_2 emitted by the fleet. Then, for every 1400 MT year^{-1} CO_2 produced in FFOV, 520 MT H_2O year^{-1} is produced. (The use of octane as a chemical representation of vehicle fuel overestimates water vapor produced by FFOV.)

As a result, a HFCV fleet may decrease water vapor emissions from 520 to 540 MT H_2O year^{-1} with a FFOV fleet to 510 MT year^{-1} H_2O for a HFCV, a slight decline. The actual change in water vapor emission depends on the ratio of efficiencies (or fuel consumption) of the vehicle fleets. Finally, if water vapor emissions were genuinely an environmental concern, a HFCV fleet could be designed to completely eliminate water vapor emissions from vehicles to zero. A HFCV fuel cell stack operates at low temperatures (∼80 °C), such that water vapor in the stack's exhaust gases could be easily condensed to liquid water.

To summarize, any HFCV fleet scenario may result in a slight decrease in water vapor emission from the vehicles, depending on the relative efficiencies of the HFCV and FFOV. However, overall water vapor emission may increase slightly due to the production of water at upstream conventional power plants that are needed to provide electricity for hydrogen compression and coal gasification. At the same time, a HFCV fleet could be designed to produced no water vapor emissions, only liquid water as a product. Hybrids also reduce water vapor emission because of their lower fuel consumption. At the same time, water vapor emission from these scenarios should be benchmarked against the natural global-scale emission rate of water vapor, approximately five orders of magnitude greater than that released by vehicles [1].

3.6. Net change in carbon dioxide emissions

If FFOV were replaced with HFCV, total annual U.S. emission of CO_2 is estimated to decrease by approximately 800, 1300 and 60 MT in the natural gas, wind, and coal scenarios, respectively. These numbers result in a reduction in CO_2 emission from all anthropogenic sources of 15, 24 and 1.0% in the natural gas, wind and coal scenarios, respectively. The natural gas and coal scenarios can achieve more significant CO_2 reductions if the carbon is sequestered, although this might be more practical for a centralized plant than for decentralized ones. Compared with FFOV, HFCV would produce some additional CO_2 due to the electric power required for the compression and processing of hydrogen, but less CO_2 on the road during vehicle operation and during direct fuel processing in the H_2 supply chain, as shown in Table 11.

An important result from this analysis is that CO_2 emission could be reduced significantly even if the hydrogen

Table 11

Carbon dioxide (CO_2) emission (MT year^{-1})	1999 vehicle fleet	Hybrid electric ICE	HFCV and natural gas	HFCV and wind	HFCV and coal
On-road vehicles and upstream H_2 supply	1371	1055	449	0	1136
Electric power plants	2231	2231	2356	2356	2403
Other sources	1698	1698	1698	1698	1698
Total	5300	4984	4503	4054	5237

economy relies on a fossil fuel such as natural gas for hydrogen production, without carbon sequestration. The primary reasons for this are: (1) a high energy conversion efficiency in converting natural gas to hydrogen via the steam reforming reaction, (2) a retention of the majority of the energy in natural gas fuel within the hydrogen bonds of the hydrogen fuel, (3) a relatively high steam to carbon ratio in the production of natural gas such that a large percentage of the mass of hydrogen originates from water, (4) a high energy conversion efficiency at the fuel cell from the chemical energy of the hydrogen fuel to electricity, (5) higher efficiencies with electric drive trains compared with mechanical ones, and (6) a relatively low carbon to hydrogen ratio in natural gas fuel ($C_nH_{3.8n}N_{0.1n}$) compared with gasoline ($C_nH_{1.87n}$) per molecule and per unit of energy [35]. Gasoline has approximately 1.6 mol C/J fuel compared with 1.3 mol C/J fuel for natural gas, on a LHV basis.

3.7. Net change in greenhouse gas emissions

Figs. 8 and 9 show the spatial distribution of emitted greenhouse gases CH_4 and CO_2. Fig. 8 shows the CH_4 emission from all anthropogenic sources by latitude and longitude for the hybrid, natural gas, wind, and coal cases, relative to the FFOV base case. The figures reflect a 4% decrease in CH_4 emission in the hybrid scenario, a 21% increase in the natural gas-HFCV scenario, and the 13% decrease in the wind and coal scenarios. Fig. 9 shows the location of CO_2 emissions from on-road vehicles, in the H_2 fuel supply chain, and from power plants, combined. Not included are other anthropogenic sources, which are the same for all scenarios. The figures reflect a decrease of 9, 22, 35 and 2% in the hybrid, natural gas, wind, and coal HFCV scenarios, respectively.

We quantify the environmental impact of emissions related to global warming by calculating the carbon dioxide equivalent (the $CO_{2\,\text{equivalent}}$) of a mixture of emitted gases and particles. The $CO_{2\,\text{equivalent}}$ is defined as the CO_2 mass that would warm the Earth to an equal extent as that mixture of emissions it refers to. $CO_{2\,\text{equivalent}}$ quantifies the warming effect of different quantities and types of emissions. We developed the following equation to describe the $CO_{2\,\text{equivalent}}$ over a 100-year period: [92,1]

$$CO_{2\,\text{equivalent}} = m_{CO_2} + 23m_{CH_4} + 296m_{N_2O} + \alpha(m_{OM\_2.5} + m_{BC\_2.5}) - \beta[m_{SULF\_2.5} + m_{NIT\_2.5} + 0.40\,m_{SO_x} + 0.10\,m_{NO_x} + 0.05\,m_{VOC}]. \quad (14)$$

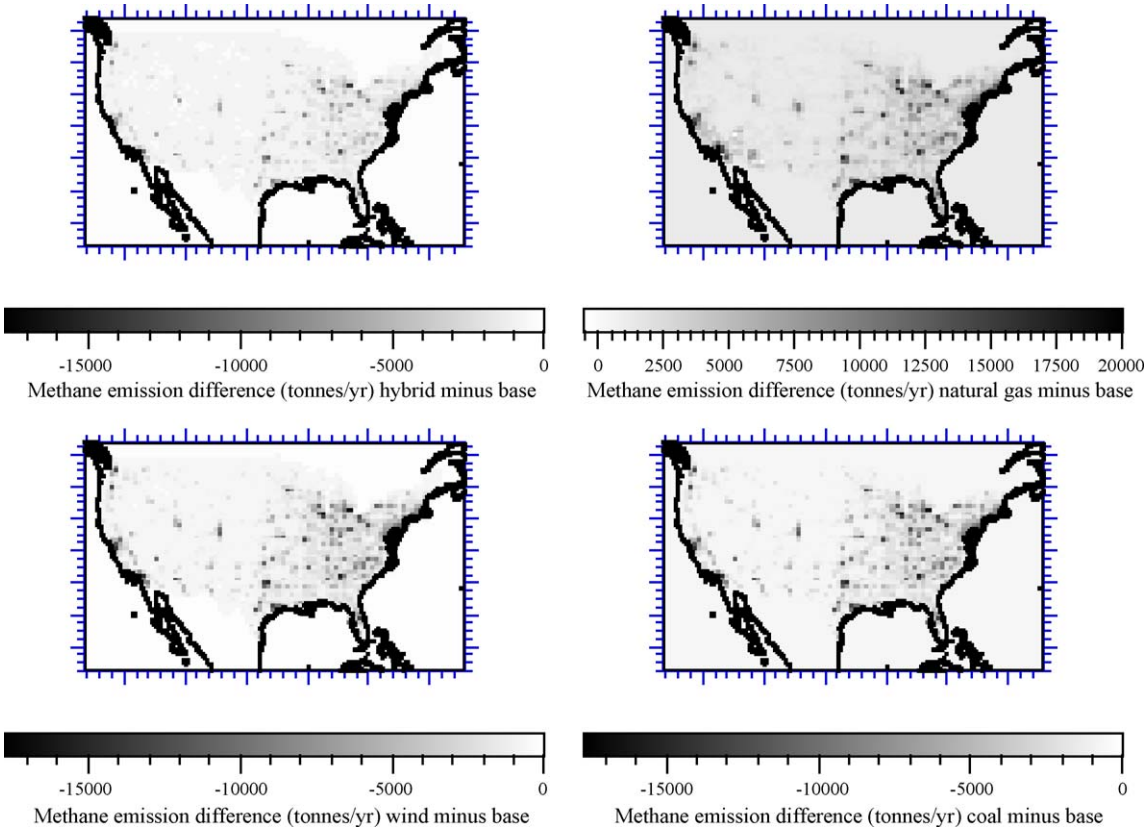

Fig. 8. (a) Spatial distribution of the difference in methane (CH_4) emissions between a hybrid electric fossil fuel on-road vehicle (FFOV) fleet scenario and the base case (1999 FFOV) scenario, (b) same as (a), except the comparison is between a hydrogen fuel cell vehicle fleet (HFCV) where the hydrogen fuel is produced from natural gas fuel and then contrasted against emissions from the base case, (c) same as (b), except the hydrogen is derived from wind, (d) same as (b), except the hydrogen is derived from coal. The scales are the same for each figure except in (b) the natural gas case, due to the increase in methane in this case.

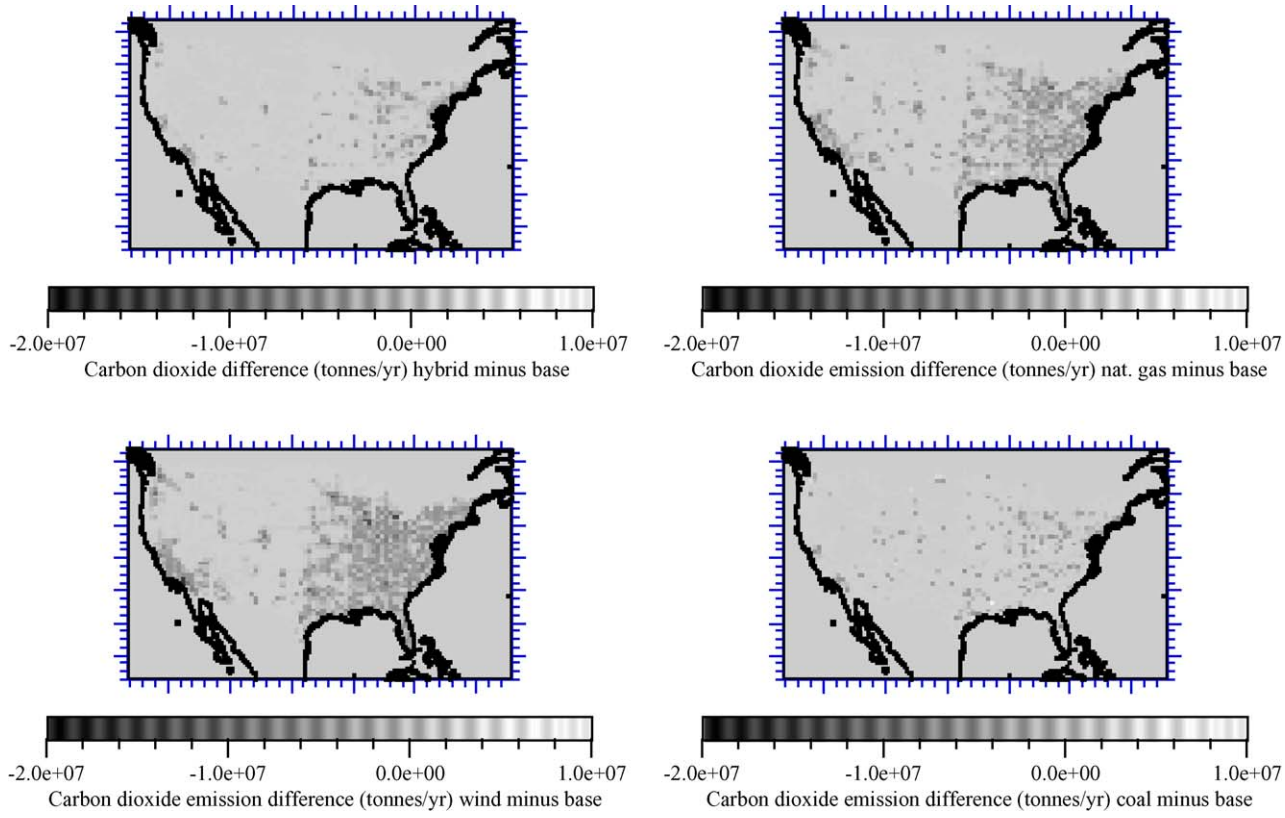

Fig. 9. (a) Spatial distribution of the difference in carbon dioxide (CO_2) emissions between a hybrid electric fossil fuel on-road vehicle (FFOV) fleet scenario and the base case (1999 FFOV) scenario, (b) same as (a), except the comparison is between a hydrogen fuel cell vehicle fleet (HFCV) where the hydrogen fuel is produced from natural gas fuel and then contrasted against emissions from the base case, (c) same as (b), except the hydrogen is derived from wind, (d) same as (b), except the hydrogen is derived from coal. The scales are the same for each figure.

The term m is the mass of each gaseous or particle species emitted. For example, $m_{OM\,2.5}$ refers to the mass of organic matter 2.5 μm in diameter and smaller. We report $CO_{2\,equivalent}$ highs for $\alpha = 191$ and $\beta = 19$, and $CO_{2\,equivalent}$ lows for $\alpha = 95$ and $\beta = 191$, reflecting the range of these coefficients. The species with positive coefficients warm the Earth and ones with negative coefficients cool it. The coefficients (23, 296, α, and β) represent the global warming potential (GWP) of each emission over a 100-year period, which estimates the relative global warming contribution of a unit mass of a particular emission compared to the emission of a unit mass of CO_2. For example, over a 100-year period, CH_4 is estimated to have a global warming effect on the climate 23 times greater than that of CO_2 because it selectively absorbs infrared radiation and then re-emits it back to Earth more readily [93]. The formula does not consider hydrogen or water vapor because hydrogen's global warming potential (if any) is still being determined by researchers and anthropogenic water vapor is a fraction of the total from global natural sources.

Based on this calculation, replacing the U.S. conventional fossil fuel vehicle fleet with hybrid electric vehicles or with HFCV with their fuel derived from natural gas, wind or coal may reduce the potential global wanning climate effect of combined emissions from these scenarios by approximately 6, 14, 23 and 1%, respectively, as shown in the last two rows of Table 10. These rows show high and low estimates for the change in $CO_{2\,equivalent}$ based on high and low coefficients. For reducing the global warming effect, the most attractive scenario is wind, followed by natural gas.

Although in the natural gas scenario CH_4 emission increased due to leakage, the potential global warming effect of the combined gases was still lower than in the base case. Considering only CO_2, the mass of CO_2 emitted would decrease by 15%, as shown in the forth to last row of Table 10. However, in the combined analysis of CO_2, CH_4, and other greenhouse gases, the mass of $CO_{2\,equivalent}$ would decrease by between 13 and 14%, as shown in the last rows of Table 10. Therefore, the increase in CH_4 emission through leakage did not negate the decrease in CO_2 emission in terms of the potential global warming potential of the combined gases. The 1% methane leakage had a small effect (1%) on changing the CO_2 equivalent effect of the gases. Therefore, the second most attractive option for reducing greenhouse gas emission is the natural gas scenario.

3.8. Analysis of uncertainties

The reductions in air pollution found here were insensitive to the energy efficiency performance characteristics of

HFCV and upstream hydrogen supply chain technologies. The primary driver behind the reduction in air pollution was the reduction in emission from FFOV themselves. Air pollution reductions could become more sensitive to upstream hydrogen supply chain technologies if prototype coal gasification plants for hydrogen production prove to emit a greater quantity of harmful pollutants than DOE computer simulation studies suggest.

Reductions in air pollution are slightly sensitive to the precision of emission estimates in the NEI. However, the uncertainty in reported NEI emissions has never been calculated due to the complexity of the database [94]. Uncertainty in reported particle emission in the NEI is probably greater than for gases. Particle emissions are probably underestimated. However, even if reported emissions in the NEI were a significant percentage greater or less than the actual values, this error would have little effect on our fundamental conclusions.

The results of this analysis with respect to emission of CO_2, H_2, and H_2O are sensitive to HFCV energy efficiency characteristics, primarily the electrical efficiency of the vehicles and the steam to carbon ratio used in hydrogen production. The electrical efficiency of HFCV could reasonably vary between a range of 36 and 56% of the LHV of hydrogen fuel, depending on technological progress, economics, vehicle design, and the particular drive cycle the vehicle is subjected to. The steam-to-carbon ratio could vary for either natural gas steam reforming or coal gasification depending on process plant design. By contrast, the tank-to-wheel efficiency of the current vehicle fleet – 16% – and the well-to-tank efficiency of the current gasoline and diesel fuel supply chain – 88% – were not significant sources of uncertainty.

4. Conclusion

This study examined the potential change in emissions and energy use from replacing fossil-fuel on-road vehicles with hybrid electric vehicles or hydrogen fuel cell vehicles. For the HFCV scenarios, this study analyzed the resultant emissions and energy usage from three different hydrogen production methods: (1) steam reforming of natural gas, (2) electrolysis powered by wind energy, and (3) coal gasification. The net change in emissions was derived using the EPA's National Emissions Inventory and a life cycle assessment of the different hydrogen fuel supply chains.

Three important results can be highlighted from this analysis. First, for a range of reasonable HFCV efficiencies and methods of producing hydrogen, replacing the current fossil fuel on-road vehicle fleet (FFOV) with a hydrogen fuel cell vehicle fleet would result in a significant reduction in air pollutant emission, even in comparison with a switch to hybrid-electric gasoline vehicles, due to the elimination of the combustion products at the internal combustion engine and the reduction of upstream petroleum processing emissions. In all HFCV scenarios, the net quantity of most types of emissions associated with air pollution would decrease, including nitrogen oxides (NO_x), volatile organic compounds (VOCs), particulate matter ($PM_{2.5}$ and $PM_{2.5–10}$), ammonia (NH_3), and carbon monoxide (CO). Similar reductions in air pollutant emission were achieved with a fossil fuel such as natural gas as with a renewable source such as wind. Second, replacing FFOV with hybrid electric vehicles or with HFCV with their fuel derived from natural gas, wind or coal would reduce the global warming impact of greenhouse gases and particles (measured in CO_2 equivalent emission) by about 6, 14, 23 and 1%, respectively. Assuming reliance on conventional power plants for electricity needed in the hydrogen supply chain, this HFCV fleet would produce some additional CO_2 emission at the power plants compared with the FFOV base case due to the electric power required for the compression of hydrogen. However, over the entire supply chain including vehicle operation, the HFCV fleet would produce less CO_2 emissions. Finally, even if HFCV are fueled by a fossil fuel such as natural gas, no carbon is sequestered, and 1% of methane in the feedstock gas is leaked to the environment, this scenario still achieves a significant 14% reduction in CO_2 equivalent greenhouse gas emission and reduced air pollution over the 1999 FFOV fleet. This result emanates from: (1) the lower quantity of carbon in natural gas per unit of fuel energy as compared with gasoline or diesel fuel, (2) a high energy conversion efficiency in converting natural gas to hydrogen via the steam reforming reactions, (3) the higher efficiencies of electric drive trains over mechanical ones, and (4) the higher efficiency and lower emission profile of fuel cell systems over internal combustion engines. All proposed scenarios – either hybrid or fuel cell – significantly reduce air pollution and global warming compared with the current fleet.

Also, four key misconceptions can be corrected. First, at realistic hydrogen leakage rates (<3%), a HFCV fleet would leak less hydrogen into the atmosphere (not more) than the current on-road vehicle fleet releases due to incomplete combustion. Second, over a range of realistic efficiencies, a HFCV fleet would emit about the same amount of water vapor as the current on-road fleet (not more) and could potentially emit none if the water vapor in the fuel cell system's low temperature exhaust was condensed. Third, although a liquid hydrogen based economy may be "leaky" in terms of both: (1) energy losses and (2) the unintentional loss of hydrogen to the atmosphere, a gaseous hydrogen based economy can be designed to be both energy efficient and low in hydrogen leakage (<3%). Finally, although hydrogen economies can be designed to be energy inefficient and highly polluting, they can also be designed to increase energy efficiency and reduce emissions, as shown by the HFCV scenarios here.

Acknowledgements

This work was sponsored by Stanford University's Global Climate Energy Project (GCEP) and the National Aeronau-

tics and Space Administration (NASA). For discussions on fuel cell technologies, the authors wish to thank S. Thomas of H_2Gen Inc., B. James of Directed Technologies Inc., C. Stone of Ballard Inc., P. Gray of Johnson Matthey Pic, R. Menar and J. Staniunas of the Fuel Cells Division of United Technologies Corporation, and B. Knight and E. Villanueva of Honda R&D. For discussions of air pollution and national emission inventories, the authors thank D. Brzezinski, S. Dombrowski, L. Driver, G. Janssen, L. Landman, H. Michaels, D. Misenheimer of the U.S. Environmental Protection Agency. For discussion of coal gasification technologies, the authors thank G. Lynch, S. Clayton and V. Der, and T. Sarkus of the U.S. Department of Energy, P. Amick of the Wabash River Coal Gasification Project at ConocoPhillips, G. Booras, N. Holt, and J. Phillips of EPRI, M. Hornick and J. McDaniel of the Polk Power Station Project at Tampa Electric Company, G. Rizeq of the Fuel Conversion Lab at GE Global Research, and R. Mitchell of Stanford's Department of Mechanical Engineering. For discussions on petroleum extraction, the authors thank R. Horne and J. Schembre of Stanford's Department of Petroleum Engineering. For discussions of environmental externalities, we thank S. Schneider of Stanford's Department of Biological Sciences, J. Sweeney of Stanford's Department of Management Science and Engineering, and M. Delucchi and J. Ogden of the Department of Environmental Science and Policy at the University of California at Davis. The authors also wish to thank C. Archer, M. Finean, G. Ketefian, J. Koomey, and E. Zedler of Stanford's Department of Civil and Environmental Engineering, and M. Reeves of Artists-At-Law.

References

[1] M.Z. Jacobson, W.G. Colella, D.M. Golden, Cleaning the air and improving health with hydrogen fuel-cell vehicles, Science 308 (5730) (2005) 1901–1905.
[2] http://www.epa.gov/ttn/chief/net/1999inventory.html.
[3] C.E. Thomas, I.F. Kuhn, B.D. James, F.D. Lomax, G.N. Baum, Affordable hydrogen supply pathways for fuel cell vehicles, Int. J. Hydrogen Energ. 23 (6) (1998) 507–516.
[4] M.Z. Jacobson, GATOR-GCMM: a global through urban scale air pollution and weather forecast model. Part 1: Model design and treatment of subgrid soil, vegetation, roads, rooftops, water, sea ice, and snow, J. Geophys. Res. 106 (2001).
[5] M.Z. Jacobson, GATOR-GCMM: Part 2: A study of day- and nighttime ozone layers aloft, ozone in national parks, and weather during the SARMAP field campaign, J. Geophys. Res. 106 (2001) 5403–5420.
[6] D.B. Myers, G.D. Ariff, B.D. James, R.C. Kuhn, Hydrogen from renewable energy sources: pathway to 10 quads for transportation uses in 2030 to 2050, The Hydrogen Program Office, Office of Power Technologies, U.S. Department of Energy, Washington, DC, Grant No. DE-FG01-99EE35099, 2003.
[7] S. Kartha, Wind and PV electrolysis, Renewable hydrogen forum: a summary of expert opinion and policy recommendations, National Press Club, Washington, DC, 1 October 2003. http://www.ases.org/hydrogen_forum03/Forum_report_c_9_24_03.pdf.
[8] A. Bauen, Renewable hydrogen and its role for vehicle refueling, Energ. World (2004).
[9] California fuel cell partnership: codes, standards and regulations. http://www.fuelcellpartnership.org/resource-otherlinks.htm.
[10] J.B. Heywood, M.A. Weiss, A. Schafer, S.A. Bassene, V.K. Natarajan, The performance of future ICE and fuel cell powered vehicles and their potential fleet impact, SAE paper series, Paper number 04P-254, 2004.
[11] The hydrogen backlash, Science, vol. 305, 2004, p. 961.
[12] I. Kuhn, S. Thomas, F. Lomax, B. James, W. Colella, Fuel processing systems for fuel cell vehicles, Report for the U.S. Department of Energy, 1997.
[13] B. James, F. Lomax, S. Thomas, W. Colella, PEM fuel cell power system cost estimates: sulfur-free gasoline partial oxidation and compressed direct hydrogen, Report for the U.S. Department of Energy, 1997.
[14] Concawe and the European Council for Automotive R&D, Well-to-wheels analysis of future automotive fuels and powertrains in the European context, Well-to-wheels Report, version lb, 2004. http://ies.jrc.cec.eu.int/Download/eh.
[15] F. Raymond, Director, BMW Group Research and Technology of Munich Germany, Hydrogen Research at the BMW Group – Our Vision of a Sustainable Individual Mobility, Mechanical Engineering Seminar Series, Department of Mechanical Engineering, Stanford University, Stanford, CA, 25 April 2005.
[16] M.A. Weiss, J.B. Heywood, E. Drake, A. Schafer, F. AuYeung, On the road in 2020: a life-cycle analysis of new automobile technologies, Energy Laboratory Report no. MIT EL-00-003, Massachusetts Institute of Technology, October 2000. http://Afee.mit.edu/publications/reports.
[17] M.A. Weiss, J.B. Heywood, A. Schafer, V.K. Natarajan, Comparative assessment of fuel cell cars, MIT LFEE 2003–2001 RP, February 2003. http://lfee.mit.edu/publications/reports.
[18] R.F. Service, Science 205 (2004) 958.
[19] T.K. Tromp, R.-L. Shia, M. Allen, J.M. Eiler, Y.L. Yung, Potential environmental impact of a hydrogen economy on the stratosphere, Science (300) (2003) 1740–1742.
[20] M.G. Schultz, T. Diehl, G.P. Brasseur, W. Zittel, Air pollution and climate-forcing impacts of a global hydrogen economy, Science 302 (2003) 624–627.
[21] R. O'Hare, S.W. Cha, W.G. Colella, F.B. Prinz, Fuel Cell Fundamentals, Chapter 11, September 2005, ISBN: 0471741485.
[22] E.M. Goldratt, J. Cox, The Goal, North River Press, New York, NY, 1992.
[23] D.H. Barnes, S.C. Wofsy, B.P. Fehlau, E.W. Gottlieb, J.W. Elkins, G.S. Dutton, P.C. Novelli, Hydrogen in the atmosphere: observations above a forest canopy in a polluted environment, J. Geophys. Res. 108 (D6) (2003) 4197, doi: 10.1029/2001JD001199.
[24] http://www.epa.gov/ttn/chief/net/1999inventory.html.
[25] Light Duty Automotive Technology and Fuel Economy Trends: 1975 Through 2004, Office of Transportation and Air Quality, Washington, DC, April 2004, EPA420-S-04-002.
[26] http://www.epa.gov/air/data.
[27] S. Gino, B. Dwight, A Contribution to Understanding Automotive Fuel Economy and Its Limits, SAE Technical Paper Series, Warrendale, PA, 2003, 2003-01-2070, p. 24.
[28] P.L. Spath, M.K. Mann, Life Cycle Assessment of Hydrogen Production via Natural Gas Steam Reforming, National Renewable Energy Lab (NREL) Technical Report, NREL, Bolder, CO, 2001.
[29] Toyota FCHV—The First Step Toward The Hydrogen Society of Tomorrow, Toyota Special Report, p. 2. http://www.toyota.co.jp/en/special/fchv/fchv_1.html.
[30] P.J. Meier, G.L. Kulcinski, Life-Cycle Energy Cost and Greenhouse Gas Emissions for Gas Turbine Power, Fusion Technology Institute, University of Wisconsin, December 2000.
[31] The Hydrogen Economy: Opportunities, Costs, Barriers, and R&D Needs, The National Research Council, Washington, DC, 2004, p. 3-3.
[32] http://www.arb.ca.gov.

[33] Harmonic average of the mileage of all vehicles in the EPA's Mobile Database for 1999.
[34] R. Venki, Hydrogen Production and Supply Infrastructure for Transportation, Workshop Proceedings: The 10-50 Solution: Technologies and Policies for a Low-Carbon Future, The Pew Center on Global Climate Change and the National Commission on Energy Policy, 2004.
[35] J.B. Heywood, Internal Combustion Engine Fundamentals, McGraw-Hill Inc., New York, NY, 1988, p. 913.
[36] Ford Motor Company, shared with Directed Technologies Inc., 2004.
[37] Personal Communication between W. Colella and S. Thomas, President, H_2Gen Innovations, July, 2004.
[38] Toyota FCHV—The First Step Toward The Hydrogen Society of Tomorrow, Toyota Special Report, p. 2. http://www.toyota.co.jp/en/special/fchv/fchv_1.html.
[39] E. Villanueva, Senior Engineer, Honda R&D Americas Inc., Presentation at Honda R&D, Torrance, CA, 22 March 2005.
[40] T. Kawanabe, Managing Director, Honda R&D Co. Ltd., Presentation at EVS-20, Long Beach, 19 November 2003.
[41] Ford Motor Company, shared with Directed Technologies Inc., 2004.
[42] Ballard Transportation Products Xcellsis^{TM} HY-80 Light Duty Fuel Cell Engine, Ballard Power Corporation, Vancouver, BC, 2004. http://www.ballard.com/pdfs/XCS-HY-80_Trans.pdf.
[43] Ballard Transportation Products A 600V300 MS High Power Electric Drive System, Ballard Power Corporation, Vancouver, BC, 2004. http://www.ballard.com/pdfs/ballardedpc600v300ms.pdf.
[44] Toyota FCHV—The First Step Toward The Hydrogen Society of Tomorrow, Toyota Special Report, p. 2. http://www.toyota.co.jp/en/special/fchv/fchv_1.html.
[45] Email communications between W. Colella and B. Knight, Vice President, Honda R&D Americas Inc., 25 March 2005 and 11 April 2005.
[46] http://world.honda.com/FuelCell/.
[47] The Hydrogen Economy: Opportunities, Costs, Barriers, and R&D Needs, The National Research Council, 2004, Washington, DC, p. 3.
[48] T. Sandy, Comparison of Natural Gas Vehicles and Hydrogen-Powered Fuel Cell Vehicles, Directed Technologies, 2003.
[49] Toyota FCHV—The First Step Toward The Hydrogen Society of Tomorrow, Toyota Special Report, p. 2. http://www.toyota.co.jp/en/special/fchv/fchv_1.html.
[50] M. Wang, Fuel choices for fuel cell vehicles: well-to-wheels energy and emissions impacts, J. Power Sources 112 (2002) 307–321.
[51] A.B. Lovins, E.K. Datta, O.-E. Bustnes, J.G. Koomey, N.J. Glasgow, Winning the Oil Endgame, Innovation for Profits, Jobs, and Security, Rocky Mountain Institute, Snowmass, Colorado, 2004, p. 65, (Figure 20).
[52] A.B. Lovins, M.M. Brylawski, D.R. Cramer, T.C. Moore, Hypercars: Materials, Manufacturing, and Policy Implications, The Hypercar Center at the Rocky Mountain Institute, Snowmass, Colorado, 1997.
[53] T. Vemersson, K. Johansson, P. Alvfors, On-board hydrogen storage for fuel cell vehicle, Proceedings of the Intersociety Energy Conversion Engineering Conference 1 (2001) 581–588.
[54] A.R. Abele, Advanced hydrogen fuel systems for fuel cell vehicles, in: First International Conference on Fuel Cell Science, Engineering, and Technology, 21–33 April, Rochester, NY, 2003.
[55] General Motors Fuel Cell Vehicle website: http://www.gm.com/company/gmability/adv_tech/400_fcv/fc_milestones.html.
[56] Toyota Motor Corporation News Release, May 16, 2005. http://www.toyota.co.jp/en/news/05/0516.html.
[57] S. Aceves, S. Perfect, A. Weisberg, Optimum Utilization of Available Space in a Vehicle through Conformable Hydrogen Tanks, LLNL, DOE Hydrogen Program FY2004 Progress Report, pp. 186–189.
[58] M.A. Delucchi, A Lifecycle Emissions Model (LEM): Lifecycle Emissions from Transportation Fuels, Motor Vehicles, Transportation Modes, Electricity Use, Heating and Cooking Fuels and Materials, Institute for Transportation Studies, University of California at Davis, Davis, CA, 2003, UCD-ITS-RR-03-17, Main Report, p. 88.
[59] R. Ewald, Requirements for advanced mobile storage systems, Int. J. Hydrogen Energ. 23 (9) (1998) 803–814.
[60] G.D. Berry, S.M. Aceves, Onboard storage alternatives for hydrogen vehicles, Energy Fuels 12 (1998) 49–55.
[61] U. Bossel, Energy and the Hydrogen Economy (January 2003) 11.
[62] M.A. Zittel, Molecular Hydrogen and Water Vapor Emission in a Global Hydrogen Energy Economy, Proceedings of the 11th World Hydrogen Energy Conference, T.N. Veziroglu, C.J. Winter, J.P. Baselt, G. Kreysa (Eds.), Schon and Wetzel, Frankfurt, Germany, 1996. www.hydrogen.org/knowledge/vapour.htm.
[63] M.E. Richards, C. Blazek, C. Webster, J. Wong, L. Gambone, Compressed Natural Gas Storage Optimization for Natural Gas Vehicles, Final Report, GRI-96/0364, Gas Research Institute, Chicago, Illinois, November, 1996.
[64] S.A. Sherif, N. Zeytinoglu, T.N. Veziroglu, Int. J. Hydrogen Energ. 22 (1997) 683.
[65] A.B. Lovins, Twenty Myths About Hydrogen #E03-05, Rocky Mountain Institute, September 2003.
[66] eGrid: The Comprehensive Environmental Database on the Electric Power Industry, United States Environmental Protection Agency (U.S. EPA), Spring 2003.
[67] Original Business Plan, H_2Gen Innovations, Alexandria, VA, USA, 22304-4806, 2000. www.h2gen.com.
[68] Directed Technologies, Cost and Performance Comparison of Stationary Hydrogen Fueling Appliances, Report for the Hydrogen Program of the Office of the Department of Energy, April 2002.
[69] W. Colella, Implications of electricity liberalization for combined heat and power (CHP) fuel cell systems (FCSs): a case study of the United Kingdom, J. Power Sources 106 (2002) 397–404.
[70] W. Colella, C. Niemoth, C. Lim, A. Hein, Evaluation of the financial and environmental feasibility of a network of distributed 200 kWe cogenerative fuel cell systems on the Stanford University Campus, Fuel Cells From Fundamentals to Systems 1 (February 2005) 148–166.
[71] Personal communication between W. Colella and R. Menar, Sales Manager, Northwest U.S. Region, UTC Fuel Cells, 20 July 2004.
[72] Idatech U.S. Patent Numbers: 5,861,137; 5,997,594; 6,152,995; 6,221,117; 6,242,120; 6,376,113; 6,375,906; 6,383,670.
[73] W. Colella, Design considerations for effective control of an afterburner sub-system in a combined heat and power (CHP) fuel cell system (FCS), J. Power Sources 118 (May 2003) 118–128.
[74] W. Colella, Modeling results for the thermal management sub-system of a combined heat and power (CHP) fuel cell system (FCS), J. Power Sources 118 (May 2003) 129–149.
[75] Email communications between W. Colella and J. Staniunas, Engineer, United Technologies Fuel Cells Inc., 15 February 2005.
[76] J.K. Dahl, A.W. Weimer, A. Z'Graggen, A. Steinfeld, Two-dimensional axi-symmetric model of a solar—thermal fluid wall aerosol flow reactor, J. Solar Energ. Eng. 127 (1) (February 2005) 76–85.
[77] K. Tatsuya, K. Yoshiyasu, K. Atsushi, K. Shimizu, Hydrogen production by solar thermochemical water-splitting/methane reforming process, in: International Solar Energy Conference, 15–18 March, 2003, pp. 121–128.
[78] C. Koroneos, A. Dompros, G. Roumbas, N. Moussiopoulos, Life cycle assessment of hydrogen fuel production processes, Int. J. Hydrogen Energ. 29 (14) (November 2004) 1443–1450.
[79] Intergovernmental Panel on Climate Change 2001, Climate Change 2001: The Scientific Basis, Cambridge University Press, Cambridge, UK, 2001.
[80] M.R. Harrison, T.M. Shires, J.K. Wessels, M.R. Cowgill, Methane Emissions from the Natural Gas Industry, United States Environmental Protection Agency (U.S. EPA), National Risk Manage-

ment Research Laboratory, Research Triangle Park, NC, 27711, EPA/600/SR-96/080, 1997.
[81] DTI Review of Energy Sources, British Electricity Grid.
[82] National Renewable Energy Laboratory (NREL), Technology Brief: Analysis of current-day commercial electrolyzers, NREL/FS 560-36705, September 2004.
[83] M.Z. Jacobson, G.M. Masters, Exploiting wind versus coal, Science 293 (2001) 1438.
[84] G.M. Masters, Renewable and Efficient Electric Power Systems, Wiley-IEEE Press Inc., New York, NY, 2004.
[85] General Electric, Wind Energy website, 2005. http://www.gepower.com/businesses/ge_wind_energy/en/products.htm.
[86] Kirk-Othmer, Encyclopedia of Chemical Technology, fourth ed., vol. 6, pp. 541–568.
[87] Gasification Plant Cost and Performance Optimization, U.S. Department of Energy, Washington, DC, 2003, DE-AC26-99FT40342 (Chapter V and Appendix H, Subtask 1.7—Coal to Hydrogen Plant).
[88] T.C. Bond, D.G. Streets, K.F. Yarber, S.M. Nelson, J.-H. Woo, Z. Klimont, A Technology-Based Global Inventory of Black and Organic Carbon Emissions from Combustion, Journal of Geophysical Research, vol. 109, D14203, doi: 10.1029/2003JD003697, 2004.
[89] Understanding the Health Effects of Components of the Particulate Matter Mix: Progress and Next Steps, HEI Perspectives, Health Effects Institute, Boston, MA, April 2002.
[90] J.A. Turner, Science 305 (2004).
[91] EIA—http://www.eia.doe.gov/cneaf/alternate/page/datatables/table10.html.
[92] M.Z. Jacobson, The climate response of fossil-fuel and biofuel soot, accounting for soot's feedback to snow and sea ice albedo and emissivity, J. Geophys. Res., 109, D21201, doi: 10.1029/2004JD004945, 2004.
[93] J.T. Houghton, Y. Ding, D.J. Griggs, M. Noguer, P.J. Van Der Linden, X. Dai, K. Maskell, C.A. Johnson, Climate Change 2001 The Scientific Basis, Cambridge University Press, Cambridge, UK, 2001, p. 388, ISBN: 0521 80767 0.
[94] Email communication between W. Colella and D. Brzezinski, Environmental Protection Agency (EPA), Office of Transportation and Air Quality, Assessment and Standards Division, 22 December 2004.